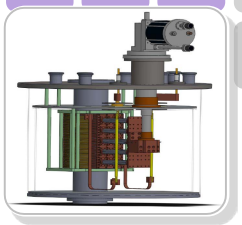

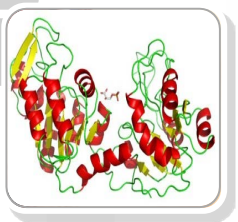

Development Progress of a 9.4 T 100 mm Metal-Clad No-Insulation All-REBCO High-Resolution NMR Magnet Cooled by Conduction

SangGap Lee[1], Seungyong Hahn[2], Sangwon Yoon[3], Jae Young Jang[1], Young Jin Hwang[1], Jun Hee Han[1], Jaemin Kim[3], Kang Hwan Shin[3], Kyekeun Cheon[3], Hunju Lee[3], Sehwan In[4], Yong-Ju Hong[4], Hankil Yeom[4], Kwanglok Kim[5], Kwangmin Kim[5], Min Cheol Ahn[6]

[1] Korea Basic Science Institute, Daejeon, Korea

[2] Seoul National University, Korea

[3] SuNAM, Gyeonggi, Korea

[4] Korea Institute of Machinery & Materials, Daejeon, Korea

[5] National High Magnetic Field Lab, FSU, Florida, USA

[6] Kunsan National University, Korea

Project's Milestones up until ASC2016

- Launched the project (Aug. 2014).
- Decided to apply SuNAM's stainless-steel-clad (thickness ~ 1-2 um) REBCO tapes (Jun. 2015).
- Delivered first-ever the Metal-Clad No-Insulation All-REBCO Magnet, called MC-NI DEMO, as a large-scale user magnet (Feb. 2016)
- Found DEMO is field-chargeable > 10 times faster than its NI counterpart (Mar. 2016).
- Succeeded in detecting a NMR signal (Jul. 2016).
- Discovered first-ever a feasibility that metallic cladding can be a new knob for mitigation of screening currents (Aug. 2016).
- As-fabricated field homogeneity of ~ 830 ppm at 10mmDSV (Aug. 2016).

Progress of 9.4 T 100 mm Metal-Clad NI NMR Magnet

- The magnet was designed by NHMFL (May, 2016), constructed by SuNAM and KIMM, and is almost at the stage of final assembly before the cryogen-free cooling.
- Will be tested by KBSI and field-mapped and ferro-shimmed by KBSI and KNU.
- Adopted resistive Metallic-cladding (MC) No-Insulation (NI) and Multi-Width techniques ensuring self-protecting and enhanced field performance.
- Charging test completed at LN2 temperature and magnetic field of 1.7 T generated

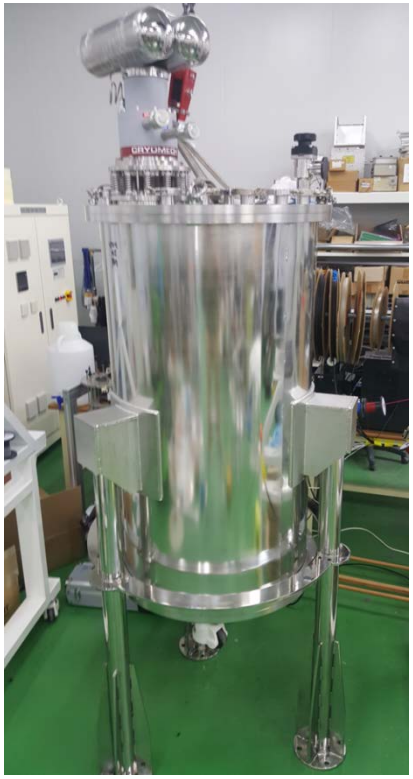

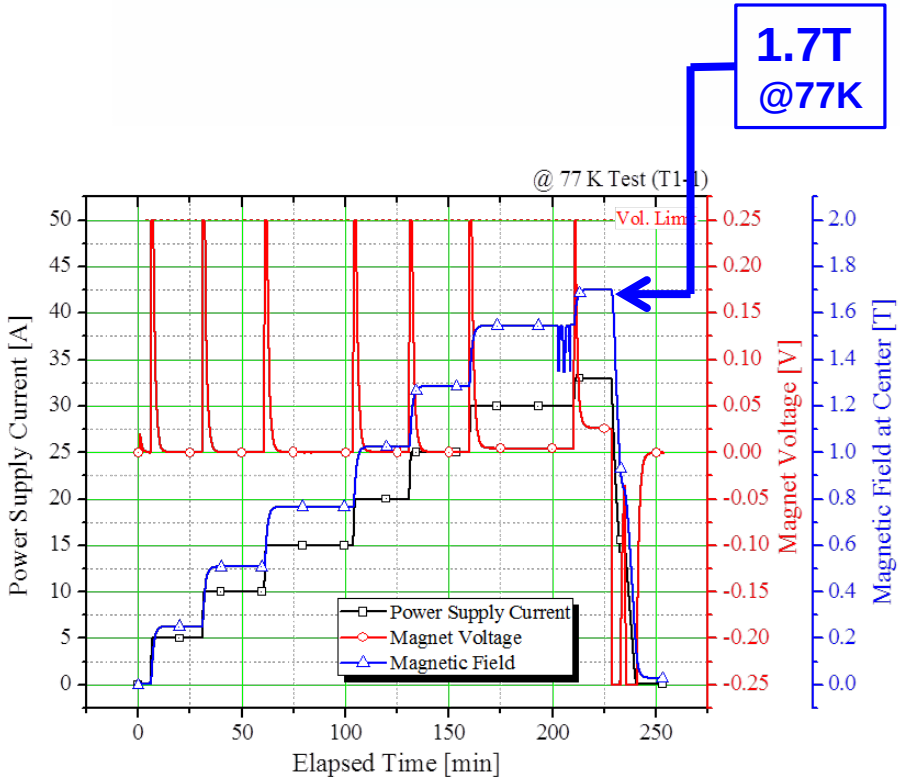

REF 1: K. L. Kim, S. Yoon, K. Cheon, J. Kim, H. Lee, S. Lee, D. L. Kim and S. Hahn, "400-MHz/60-mm All-REBCO Nuclear Magnetic Resonance Magnet : Magnet Design," IEEE Trans. Appl. Supercond., vol. 26, no. 4, 4302604, June 2016

DEMO : 3 T 100 mm MC-NI All-REBCO Magnet

- Delivered a 3 T 100 mm MC-NI All-REBCO Magnet, as a proto-type, called DEMO (Feb. 2016).
- Designed by NHMFL (May, 2015), constructed by SuNAM & KIMM, and tested by KBSI.
- Under field-mapping and ferro-shimming by KBSI and KNU : field homogeneity was ~ 830 ppm (@ 10mm DSV) as fabricated and as of now ~ 50 ppm (@ 10mm DSV).
- First-ever attempt to verify the feasibility of metal-clad NI all-REBCO magnet as a large-scale high-field DC user magnet

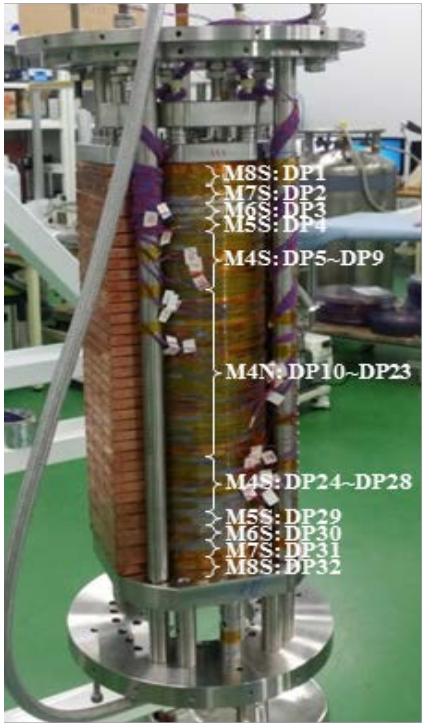

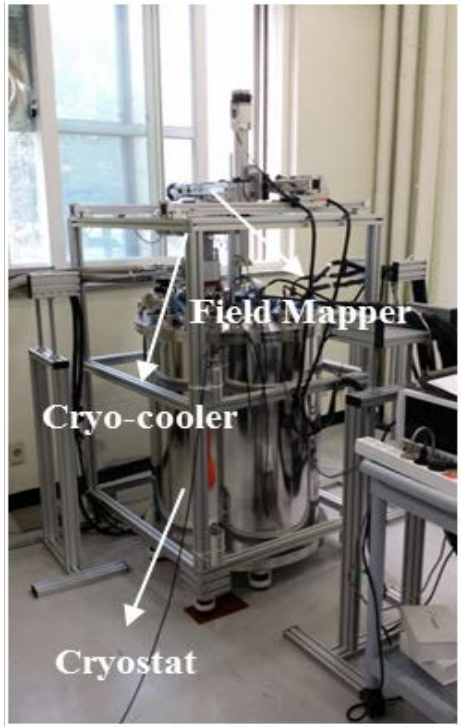

Parameters	
HTS conductor	SuNAM GdBCO
Magnetic field	> 3.0 [T]
Operating temperature	< 20 [K]
Operating current	201 [A]
Inductance	0.465 [H]
Warm bore diameter	64 [mm]

REF 1: Y. J. Hwang et al., "A Study on Mitigation of Screening Current Induced Field with a 3-T 100-mm Conduction-Cooled Metallic Cladding REBCO Magnet," IEEE Trans. Appl. Supercond., vol. 27, no. 4, 4701605, June 2017

REF 2: J. Y. Jang et al, "Design, Construction and 13 K Conduction-Cooled Operation of a 3 T 100 mm Stainless Steel Cladding All-REBCO Magnet," 2017, Supercond. Sci. Technol., at press: https://doi.org/10.1088/1361-6668/aa8354

Cooling Performance & Temperature Stability of DEMO

- Applied a two-stage pulse tube cryo-cooler with a cooling power of 22W @ 20 K
- Cooling down completed in about 1 and a half days
- Temperatures measured at the three locations (top, middle, bottom) of the coils stay stable well below 14 K during and after magnetic field ramping to the target current 201 A at a reasonably high rate of 0.1875 A/s.

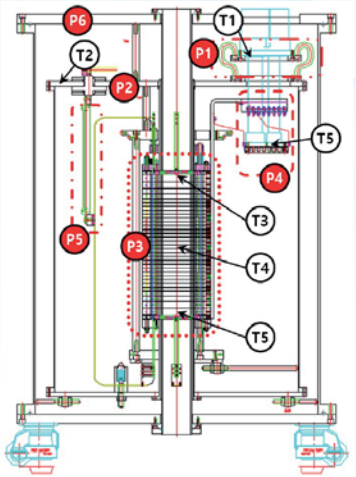

< Temperatures during cooling down >

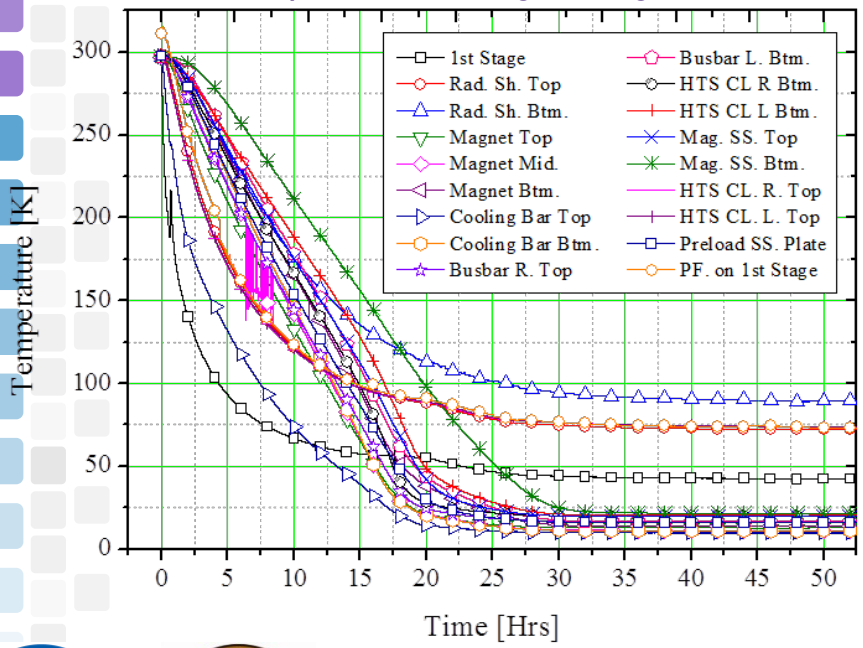

< Temperature evolution after charging completed >

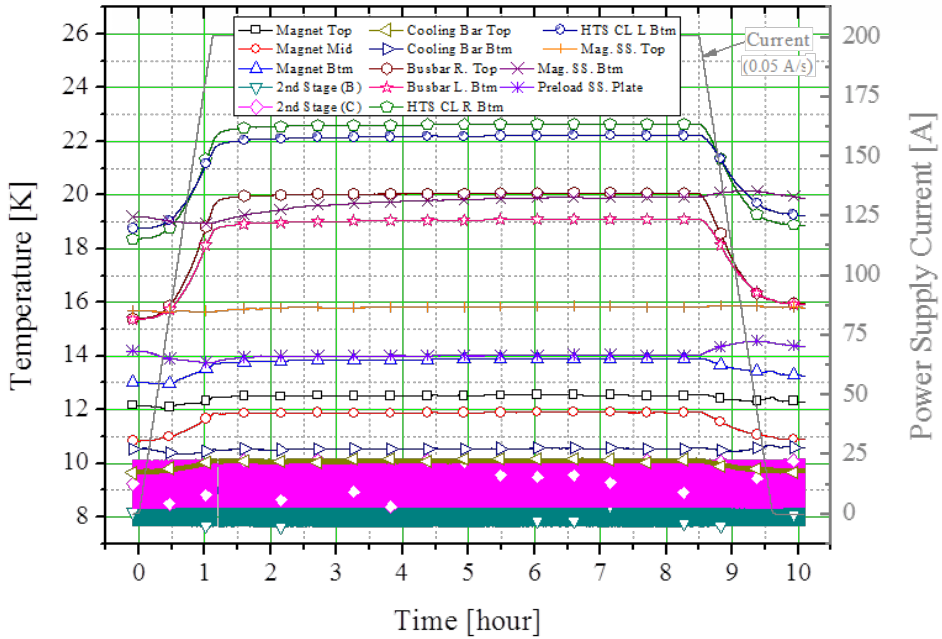

REF 1: S. In et al., "Experimental study on a conduction cooling system for an HTS NMR magnet," IEEE Trans. Appl. Supercond., vol. 27, no. 4, June 2017

Charging Delay Suppression during Field Ramping

- Charging delay during field ramping is an intrinsic drawback of the NI magnet.
- Along with the metal-clad (MC; clad thickness ~ 1-2 um) DEMO, charging delay suppressed substantially.
- Charging time constant (L/R) of the MC DEMO is 13 times smaller than that of its NI counterpart.
  - ➔ Measured *Rct* of MC magnet : about 130 [μΩ·m^2]
  - ➔ Reported *Rct* of NI counterpart magnet : about 10 [μΩ·m^2].

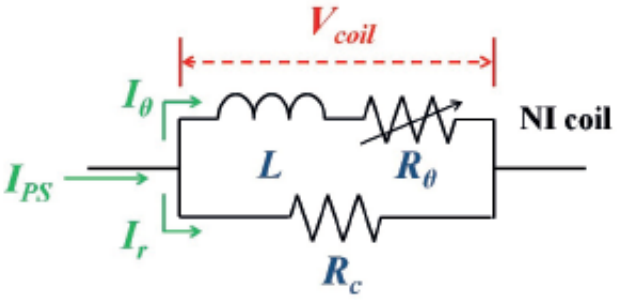

[Equivalent lumped circuit of an NI coil]

***L* : Inductance**
***Rc* : Characteristic resistance**
***Ir* : radial current through turn-to-turn contact**
***IPS* : power supply current**
***Iθ* : Spiral current**

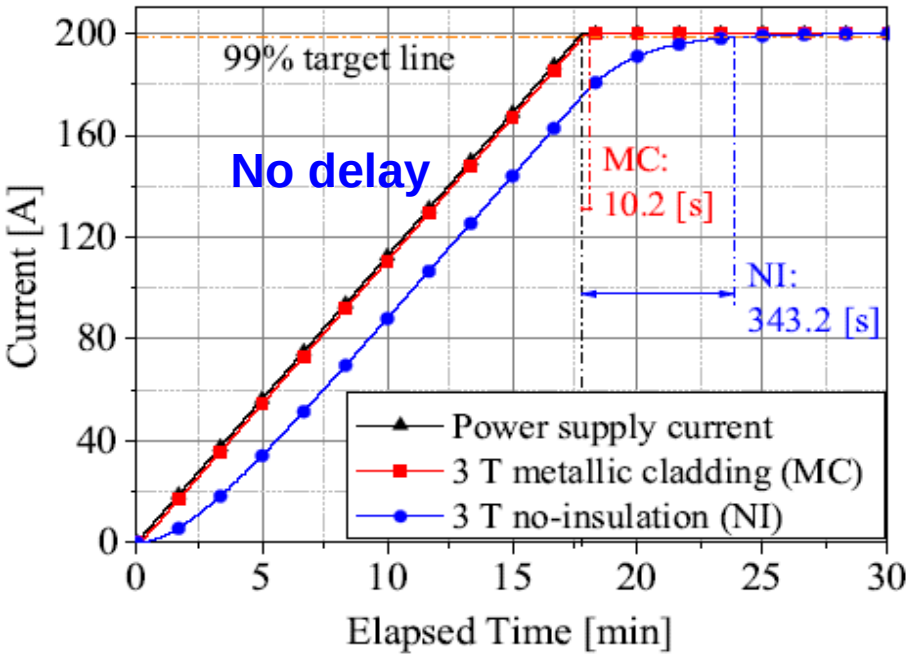

[Comparison of charging delay between the 3 T MC magnet and its NI counterpart]

Charging time constant = L/R_c ~ 10 s

REF 1: J. Y. Jang et al, "Design, Construction and 13 K Conduction-Cooled Operation of a 3 T 100 mm Stainless Steel Cladding All-REBCO Magnet," 2017, Supercond. Sci. Technol., at press: https://doi.org/10.1088/1361-6668/aa8354

Successful Detection of NMR Signal !

- Using a high-resolution 400MHz NMR hardware and operation software in development and test by KBSI and SciMedix
- 129MHz 1H NMR spectrum of water obtained at 3 T, the central field of DEMO

[3T DEMO]

[129 MHz NMR probe]

[Digital NMR transmitter/receiver]

[Full view of NMR spectrometer console]

NMR Signal Detected !

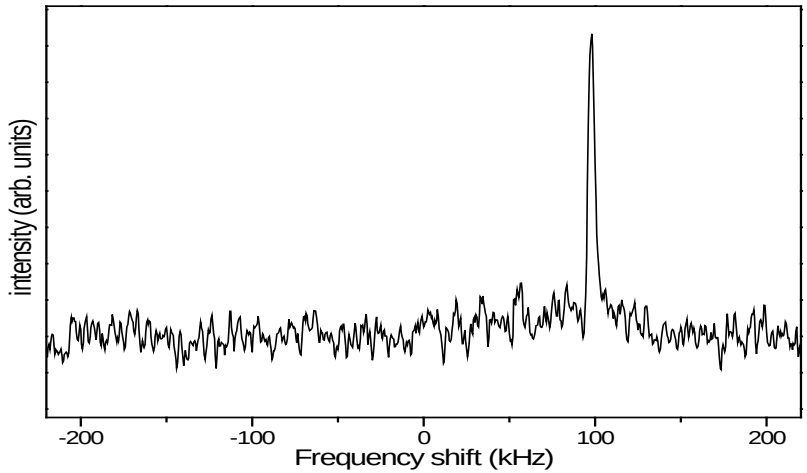

[129MHz (3T) 1H NMR spectrum of water]

Huge Drift of Screening Current Field (SCF)

- MC-NI DEMO shows a long-term drift of magnetic field, a 10-Gauss drift lasting for 8 hours or longer, which is well resolved by NMR.
- The drift is huge in viewpoint of NMR but so tiny to be resolved by Hall magnetometer.
- The drift is not a sort of charging delay due to no-insulation definitely, as the delay should complete in 10 tau (~ 100 s) after ramping up stops. Rather than charging delay, it is a field drift due to slow relaxation of screening currents.

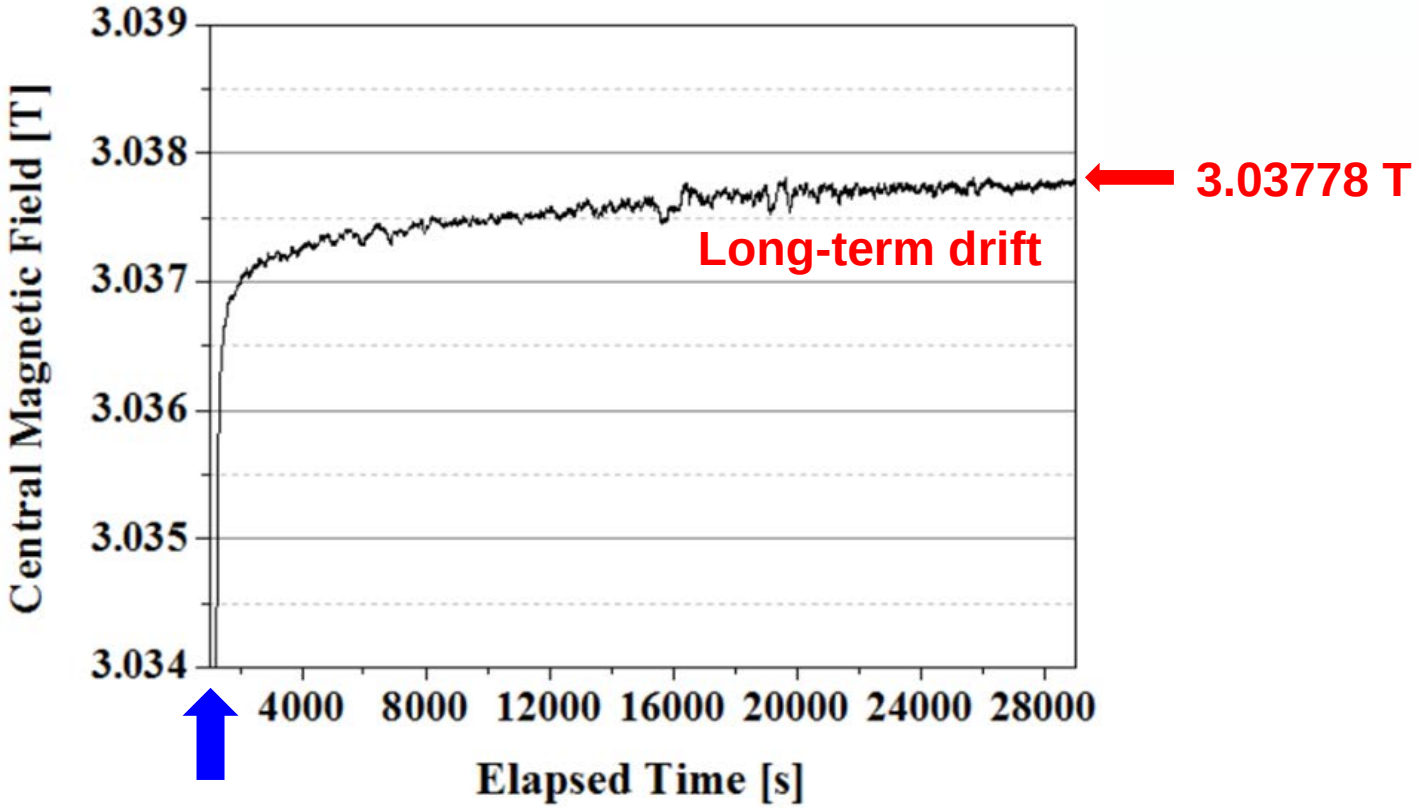

REF 1: Y. J. Hwang et al., "A Study on Mitigation of Screening Current Induced Field with a 3-T 100-mm Conduction-Cooled Metallic Cladding REBCO Magnet," IEEE Trans. Appl. Supercond., vol. 27, no. 4, 4701605, June 2017

SCF Suppression Due to Metal-Cladding Effect

- Current Sweep Cycles (CSC) is known to be effective for mitigation of SCF in insulation REBCO.
- MC DEMO shows no substantial delay in the field following CSC but NI counterpart does.
- CSC reduces the field drift effectively and increases DC field of about 100 G immediately after CSC completed.
- Various CSC takes out diamagnetic portion of the field effectively.

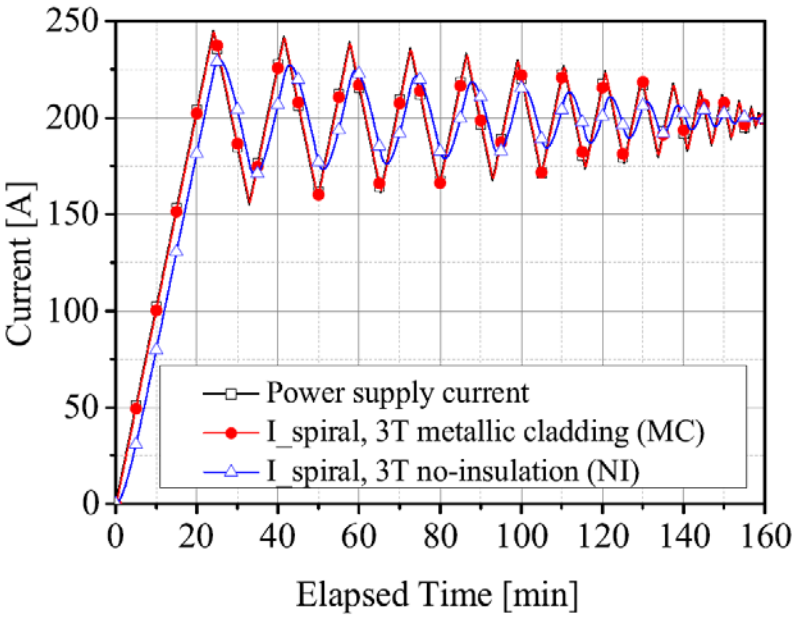

< Simulated magnetic field following CSC >

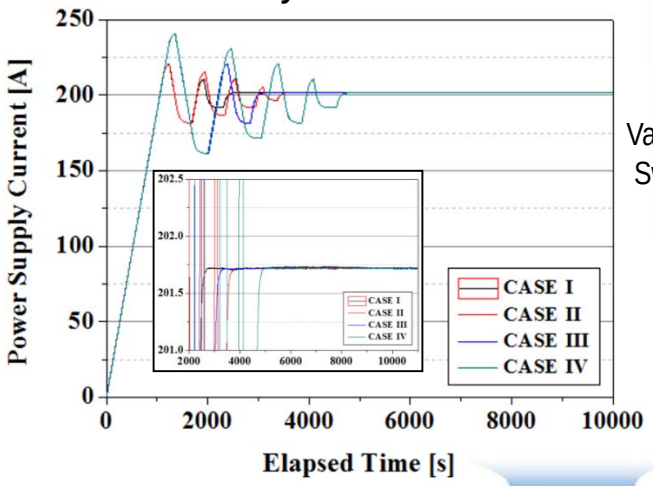

Various Current Sweep Cycles

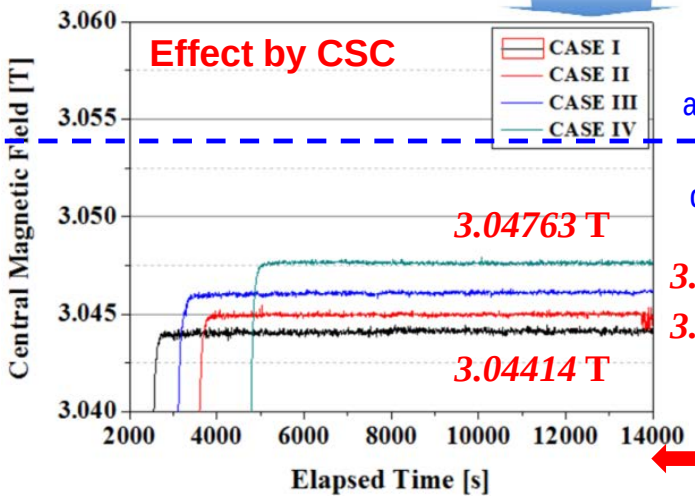

REF 1: Y. J. Hwang et al., "A Study on Mitigation of Screening Current Induced Field with a 3-T 100-mm Conduction-Cooled Metallic Cladding REBCO Magnet," IEEE Trans. Appl. Supercond., vol. 27, no. 4, 4701605, June 2017

REF 2: J. Y. Jang et al, "Design, Construction and 13 K Conduction-Cooled Operation of a 3 T 100 mm Stainless Steel Cladding All-REBCO Magnet," 2017, Supercond. Sci. Technol., at press: https://doi.org/10.1088/1361-6668/aa8354

Precision Field Mapping System

- Composed of an NMR spectrometer and a 3-D linear positioner.
- The NMR using a small volume of NMR-active sample to increase a field resolution, a high-Q tank circuit, and a high-power RF amplifier for high precision measurement.

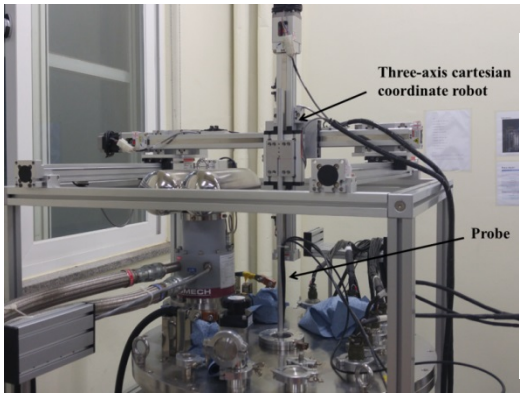

< three-axis step-motorized linear positioner >

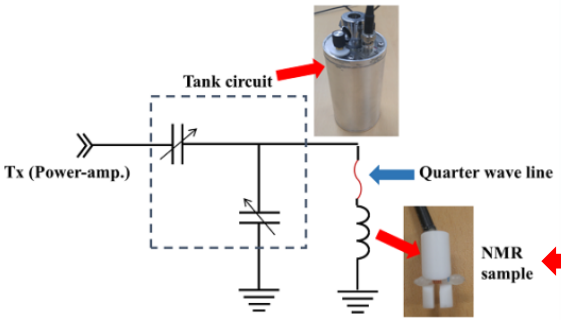

< high-Q tank circuit >

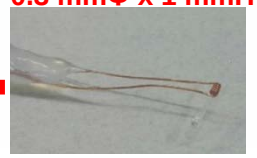

< NMR sensor >

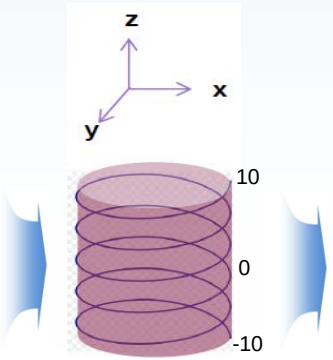

< mapping pathway >

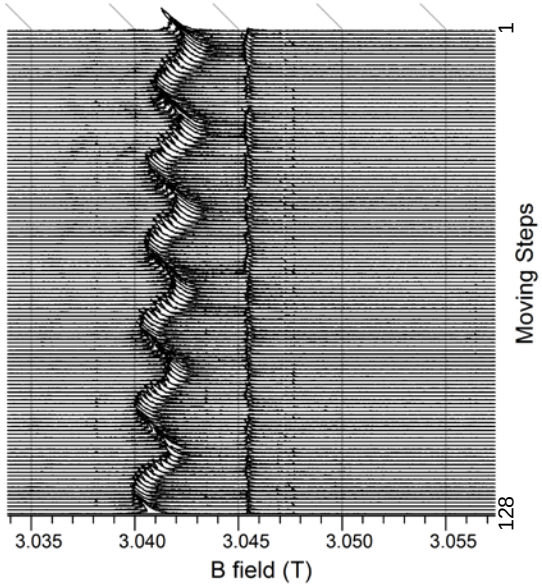

< NMR spectra along the pathway >

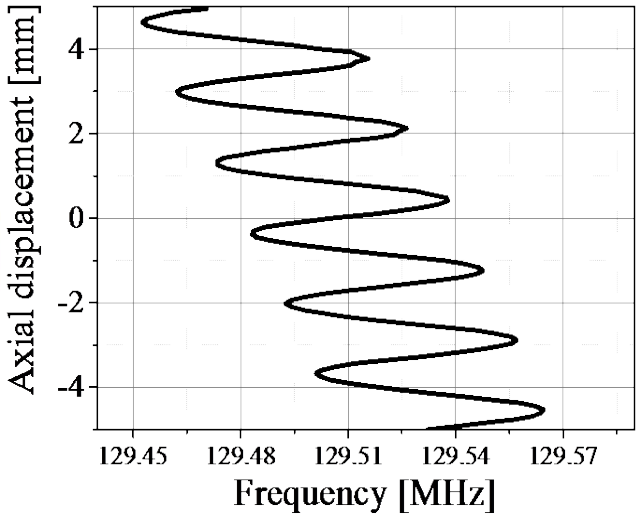

< magnetic-field map along the pathway >

Z0	128.67987	MHz
Z1	-64864	Hz/cm
X	-25126	Hz/cm
Y	-54772	Hz/cm
Z2	-23017	Hz/cm^2
ZX	-5730	Hz/cm^2
ZY	2856.5	Hz/cm^2
C2	217.98	Hz/cm^2
S2	5704.2	Hz/cm^2
Z3	-1274.7	Hz/cm^3
Z2X	7493.2	Hz/cm^3
Z2Y	432.1	Hz/cm^3
ZC2	2504.5	Hz/cm^3
ZS2	-2659.3	Hz/cm^3
C3	-407.26	Hz/cm^3
S3	1553.5	Hz/cm^3

< calculated field gradients >

REF 1: J. Y. Jang et al, Manuscript in Preparation

Design and Fabrication of Ferro-shim for DEMO

- Optimal design of an array of ferro-shims to be placed on a cylindrical surface
- Design with the structure of a concentric multiple cylindered shimming stack

	Before shim
Z0 (MHz)	128703368.5
Z1 (Hz/cm)	-48523.95
X (Hz/cm)	798.85
Y (Hz/cm)	-63964.78
Z2 (Hz/cm^2)	-2716.68
ZX (Hz/cm^2)	-11553.2
ZY (Hz/cm^2)	-3788.19
C2 (Hz/cm^2)	-2343.05
S2 (Hz/cm^2)	1691.7
Z3 (Hz/cm^3)	-2833.3
Z2X (Hz/cm^3)	-490
Z2Y (Hz/cm^3)	5044.23
ZC2 (Hz/cm^3)	-226.27
ZS2 (Hz/cm^3)	1058.06
C3 (Hz/cm^3)	2213.29
S3 (Hz/cm^3)	2254.22
ppm	634

< Mapping results >

Shim design

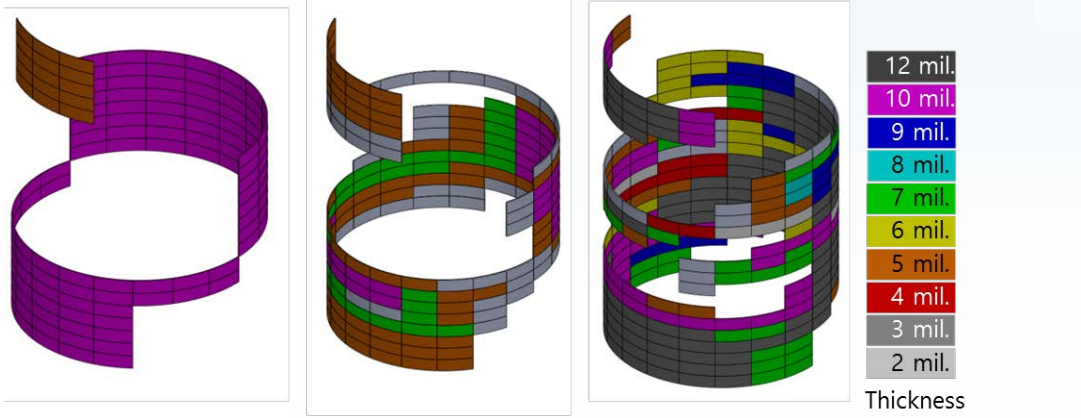

<1st try shim> <2nd try shim> <3rd try shim>

< Designs of single-cylindered ferro-shims >

Fabrication

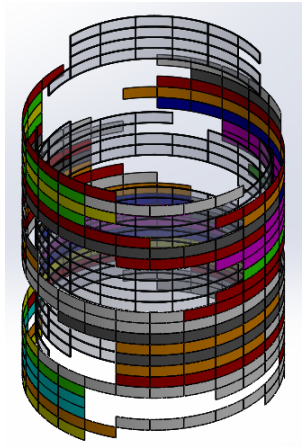

Fabrication

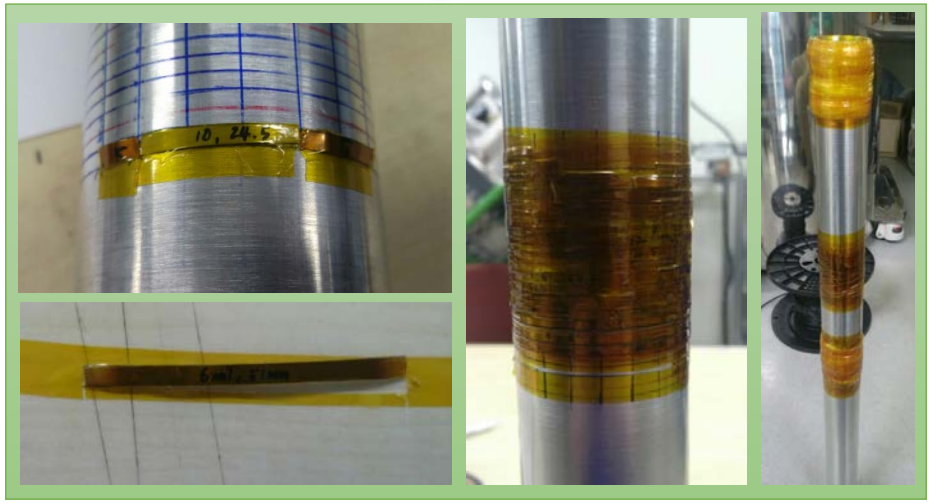

< Design of double -cylindered ferro-shims >

< Fabricated stack of ferro-shims >

REF 1: J. Y. Jang et al, Manuscript in Preparation

Evaluation of Ferro-shims – 50 ppm @ 10 mmDSV

- With a double-cylindered stack of ferroshims, ~ 50 ppm @ 10 mmDSV, the best as of now
- With single-cylindered stacks of ferroshims, best homogeneity ~ 110 ppm

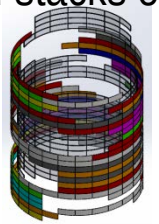

	Before Shim	Inner Shim	Inner & Outer shims
Z0 (MHz)	128.7034	128.7872	128.7439
Z1 (Hz/cm)	-48523.95	7850.8	-2520.06
X (Hz/cm)	798.85	-13170.7	-2690.52
Y (Hz/cm)	-63964.78	-11596.4	-2719.96
Z2 (Hz/cm^2)	-2716.68	4941.2	1554.95
ZX (Hz/cm^2)	-11553.2	-7658.3	2490.85
ZY (Hz/cm^2)	-3788.19	-9616.2	-3441.17
C2 (Hz/cm^2)	-2343.05	-3737	-2032.85
S2 (Hz/cm^2)	1691.7	1351.6	-1375.65
Z3 (Hz/cm^3)	-2833.3	458.7	1161.73
Z2X (Hz/cm^3)	-490	4388.3	5479.61
Z2Y (Hz/cm^3)	5044.23	623.1	6387.84
ZC2 (Hz/cm^3)	-226.27	194.9	1632.67
ZS2 (Hz/cm^3)	1058.06	584.6	-2085.69
C3 (Hz/cm^3)	2213.29	1781	505.24
S3 (Hz/cm^3)	2254.22	-643.4	-843.52
Uniformity (ppm)	**634**	168	**53.9**

<Field gradients before & after ferro-shimming>

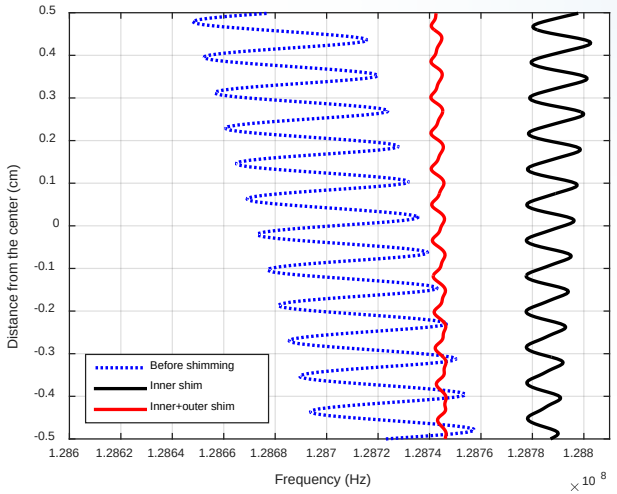

<Field map along a cylindrical helix (17mmΦx10mmH)>

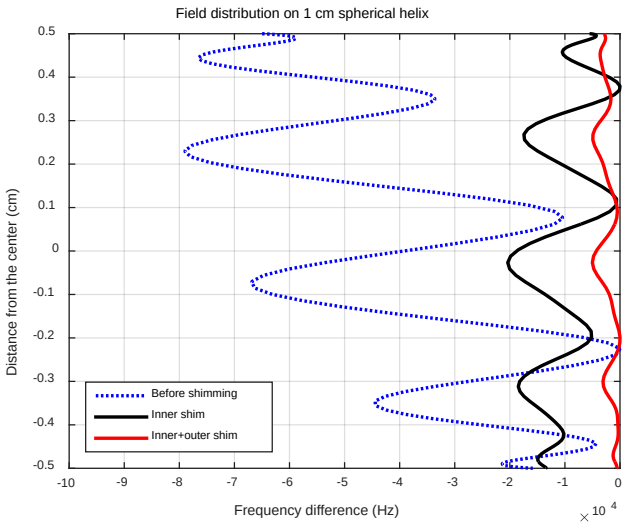

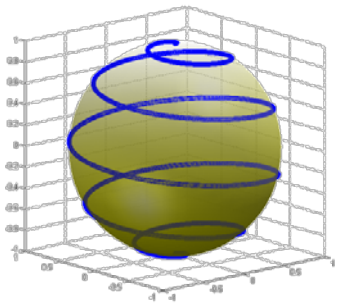

Blue: 634 ppm
Red: 53.9 ppm

<Field map on a spherical helix (Φ10mm DSV)>

REF 1: J. Y. Jang et al, Manuscript in Preparation

Reproducible Field Gradient during Ferroshimming

- After installation of ferro-shims, CSC technique was applied to reduce the SCF.
- Field mapping was repeatedly carried out to obtain a temporal dependence of field gradients with a stack of ferro-shims. Due to the efficient mitigation of SCF due to metallic cladding, calculated field gradients and homogeneity are almost the same with respect to trials.

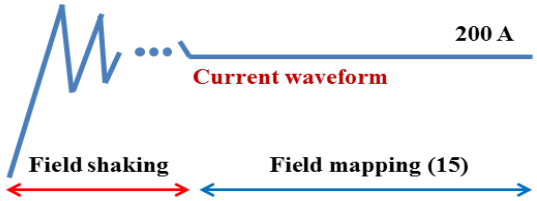

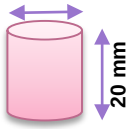

✓ **Magnetic field mapped along a helical path**

	1	2	3	4	5	6	7	8	AVG(8)	STDEV(8)
Z0	128768077.4	128767728.6	128767308	128768284	128768047	128767337.2	128766855.7	128767275.3	**128767614.2**	**496.3081359**
Z1	-371.6917822	-404.2400961	-1255.206054	-86.50404388	-395.5340494	-644.6592532	-491.270539	-518.3889728	**-520.9368488**	**337.1508833**
X	-8566.361388	-8525.149379	-8478.236926	-8624.36179	-8613.114003	-8657.8017	-8529.431501	-8418.702333	**-8551.644878**	**80.00887666**
Y	659.2793377	642.7341965	582.9658026	547.7569877	856.5229678	752.0331201	760.4224391	744.1631606	**693.2347515**	**102.9940879**
Z2	3693.926648	3837.630925	4181.220343	3500.462225	3678.045132	3824.244308	3249.451806	3974.618665	**3742.450007**	**285.4268046**
ZX	89.59081043	642.7364898	675.7283615	25.97068737	284.2213748	178.7869657	220.15021	358.5199134	**309.4631016**	**239.6515106**
ZY	-2317.385585	-2379.03501	-2170.851555	-1983.66149	-2438.565456	-2231.515674	-2281.179978	-2314.663741	**-2264.607311**	**140.2735759**
C2	314.0039997	463.6920302	426.0970298	101.8595761	283.6391078	381.563623	317.8535168	326.3960667	**326.8881188**	**109.7421117**
S2	474.8446527	825.4147751	757.3098596	605.3548961	353.5675819	455.1428101	504.8005425	393.0369021	**546.1840025**	**169.7437812**
Z3	246.4285079	1508.442237	-909.379216	407.5426303	402.569448	766.4933975	428.6482915	488.4762329	**417.4026911**	**666.2591913**
Z2X	7515.646892	6955.20751	6676.840194	7760.641613	7111.775233	7325.716556	7087.608962	6337.132383	**7096.321168**	**453.9253643**
Z2Y	839.6490975	124.7571229	374.152027	212.1074209	18.45480342	516.168125	292.8013701	437.7906403	**351.9850759**	**255.9491286**
ZC2	1166.825032	845.1496404	974.3327808	1256.457039	797.4291022	1115.692652	1135.97288	928.3850241	**1027.530519**	**164.842737**
ZS2	-3959.993538	-3804.171355	-4085.120396	-4491.788149	-3769.234769	-3846.734174	-4030.88772	-3906.20635	**-3986.767056**	**231.1906633**
C3	-105.2412993	-286.8102692	-124.7256432	35.53768968	-6.265337175	-17.54112561	-94.50524778	-89.74094493	**-86.16152219**	**98.63094009**
S3	-955.5322104	-1130.320131	-1188.942824	-973.827165	-816.4597113	-828.8565143	-988.9288692	-781.9283981	**-958.0994779**	**147.3357791**

ppm@1cm	54	56	59	52	54	56	54	54	54.8	2.1

REF 1: J. Y. Jang et al, Manuscript in Preparation

Current waveform

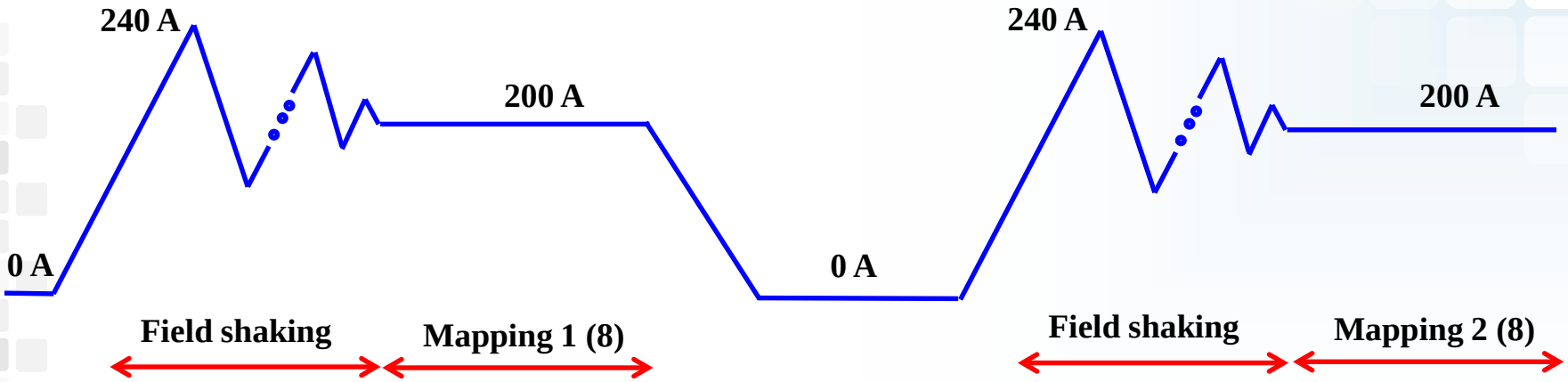

	AVG(8)	STDEV(8)
Z0	128767614.2	496.3081359
Z1	-520.9368488	337.1508833
X	-8551.644878	80.00887666
Y	693.2347515	102.9940879
Z2	3742.450007	285.4268046
ZX	309.4631016	239.6515106
ZY	-2264.607311	140.2735759
C2	326.8881188	109.7421117
S2	546.1840025	169.7437812
Z3	417.4026911	666.2591913
Z2X	7096.321168	453.9253643
Z2Y	351.9850759	255.9491286
ZC2	1027.530519	164.842737
ZS2	-3986.767056	231.1906633
C3	-86.16152219	98.63094009
S3	-958.0994779	147.3357791
ppm@1cm	54.8	2.1

[Mapping 1]

	AVG(8)	STDEV(8)
Z0	128767754.5	445.31186
Z1	-619.3431139	331.81291
X	-8601.567435	95.923899
Y	558.615116	123.53481
Z2	3581.09794	430.50188
ZX	138.6325937	225.52832
ZY	-2275.388519	152.78194
C2	235.4411415	94.718818
S2	481.1836708	133.0675
Z3	206.946477	1037.5672
Z2X	7157.465365	486.98528
Z2Y	541.7584091	472.12546
ZC2	1237.823162	282.59335
ZS2	-3856.625573	216.67724
C3	-94.23532906	153.79958
S3	-931.9529642	176.22317
ppm@1cm	54.5	2.9

[Mapping 2]

REF 1: J. Y. Jang et al, Manuscript in Preparation

Survival of DEMO after Sudden Discharge

- There were two times unexpected power supply trips during a long-term operation, which leads to sudden discharges of the magnet, yet the magnet survived without any degradation.
- An amount of power supply current leaks through the turn-to-turn contacts, which prevents local heating and consequent damage of the magnet. MC also shows NI's self-protecting behavior.

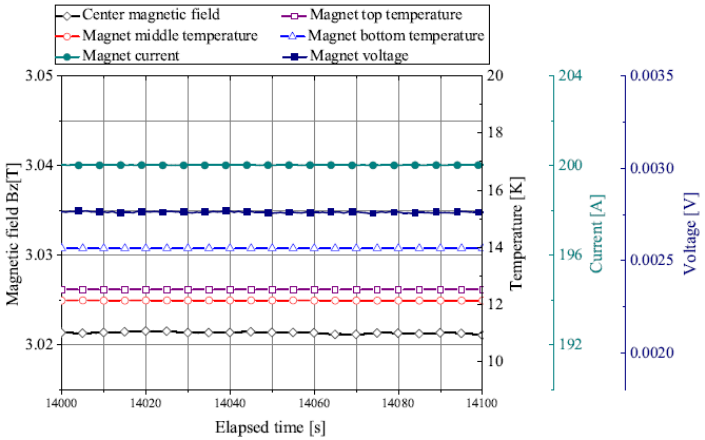

Before the sudden discharge

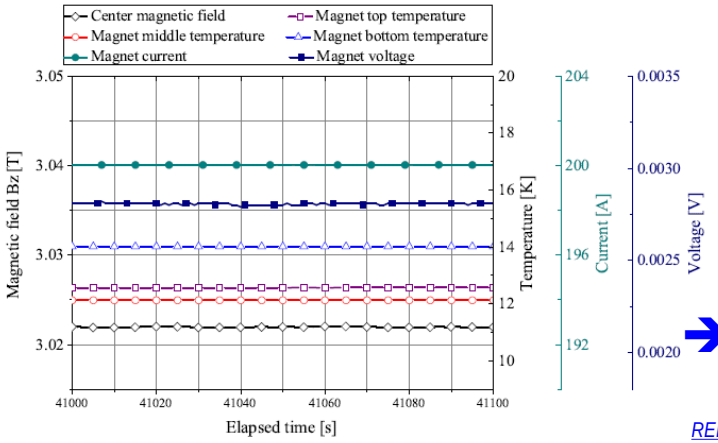

After the sudden discharge

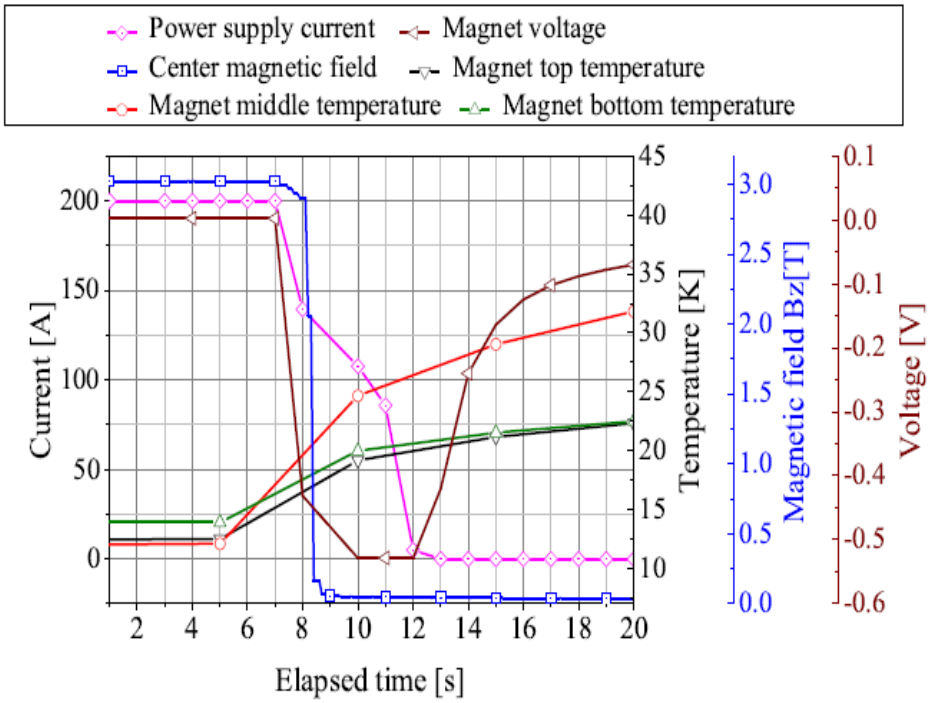

[Behavior of MC DEMO after the sudden discharge]

➔ There is no degradation or damage of the magnet

REF 1: J. Y. Jang et al, "Design, Construction and 13 K Conduction-Cooled Operation of a 3 T 100 mm Stainless Steel Cladding All-REBCO Magnet," 2017, Supercond. Sci. Technol., at press: https://doi.org/10.1088/1361-6668/aa8354

Summary

- Field homogeneity of ~ 50 ppm at 10mmDSV, the best as of now
- Calculated field gradients and homogeneity are almost the same with respect to mapping trials, maybe due to the efficient mitigation of SCF due to metallic cladding.
- We have the same field gradients and homogeneity before and after shutting down current.
- Metal-clad DEMO survived after sudden discharge.
- With 9.4 T magnet, charging test was completed at LN2 temperature and magnetic field of 1.7 T generated.

Thank You!

SangGap Lee[1], Seungyong Hahn[2], Sangwon Yoon[3], Jae Young Jang[1], Young Jin Hwang[1], Jun Hee Han[1], Jaemin Kim[3], Kang Hwan Shin[3], Kyekeun Cheon[3], Hunju Lee[3], Sehwan In[4], Yong-Ju Hong[4], Hankil Yeom[4], Kwanglok Kim[5], Kwangmin Kim[5], Min Cheol Ahn[6]

[1] Korea Basic Science Institute, Daejeon, Korea

[2] Seoul National University, Korea

[3] SuNAM, Gyeonggi, Korea

[4] Korea Institute of Machinery & Materials, Daejeon, Korea

[5] National High Magnetic Field Lab, FSU, Florida, USA

[6] Kunsan National University, Korea

Background

- **Spatial harmonics**
  - Systematical analysis of field distribution
  - Good for active shimming
  - B_z can be expressed using associated Legendre polynomials.

$$B_z = \sum_{n=0}^{\infty} \sum_{m=0}^{m=n} (n+m+1) r^n P_n^m(\cos\theta)[A_{n+1}^m \cos m\phi + B_{n+1}^m \sin m\phi]$$

    - In Cartesian coordinate,

$$B_z = A_1^0 + 2A_2^0 z - 3A_2^1 x - 3B_2^1 y + 3A_3^0 (z^2 - (1/2)(x^2 + y^2)) - 12A_3^1 zx - 12B_2^1 zy + \cdots$$

Field Gradients — *Z0* *Z1* *X* *Y* *Z2* *ZX* *ZY*

Background

Field mapping

Gathering (x, y, z, B_z) sets

→ Above equation can be solved using the sets.

→ All coefficients can be obtained.

Active shimming

- All field gradients should be as small as possible except *Z0*.
- Shim coil current can be calculated based on mapping results.

Nuclear Magnetic Resonance (NMR)

Structural Analysis of Biomolecules

- Structure analysis of Natural Substance, Proteins
- Drug design

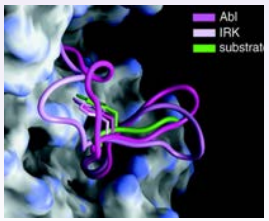

NMR's Schematic diagram

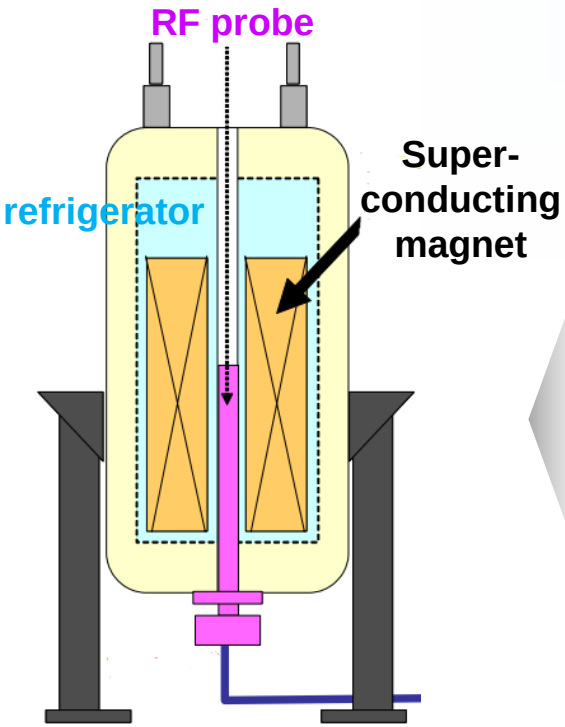

Synthesis of Macromolecules

- Functional macromolecules
- Synthetic Compound

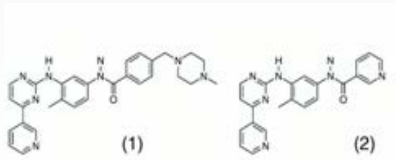

NMR signals can be generated by applying radio-frequency electromagnetic wave to a nuclear-spin sample in magnetic field.

Nuclear Magnetic Resonance (NMR)

^{1}H-^{15}N HSQC Spectrum

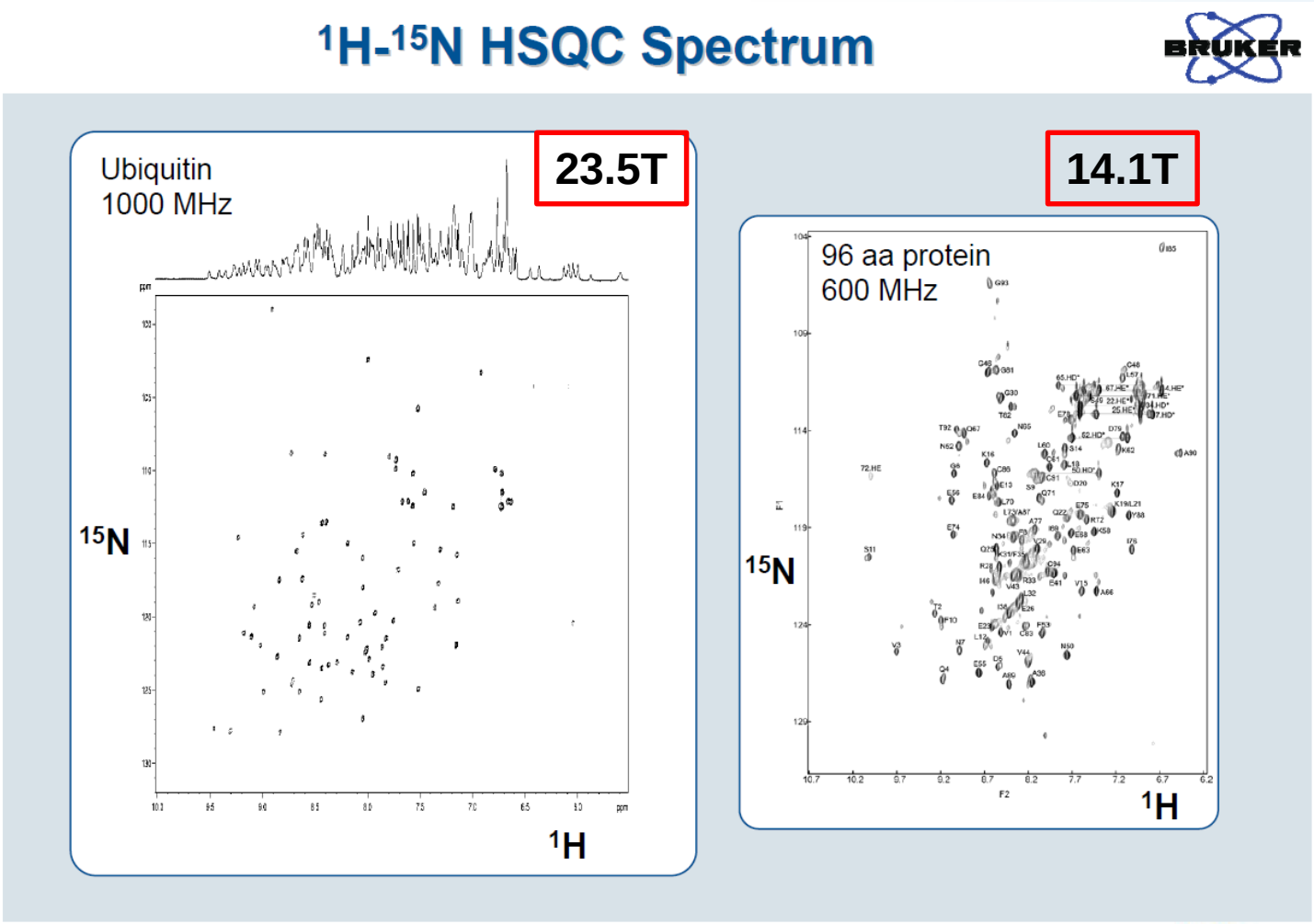

Rainer Kerssebaum, "NMR now and then - Sensitivity, Magnets, Technology" EURACT-NMR Workshop, Karsruhe, Germany (2010)

Higher magnetic field => Better spectral resolution

Benefits with HTS Wires

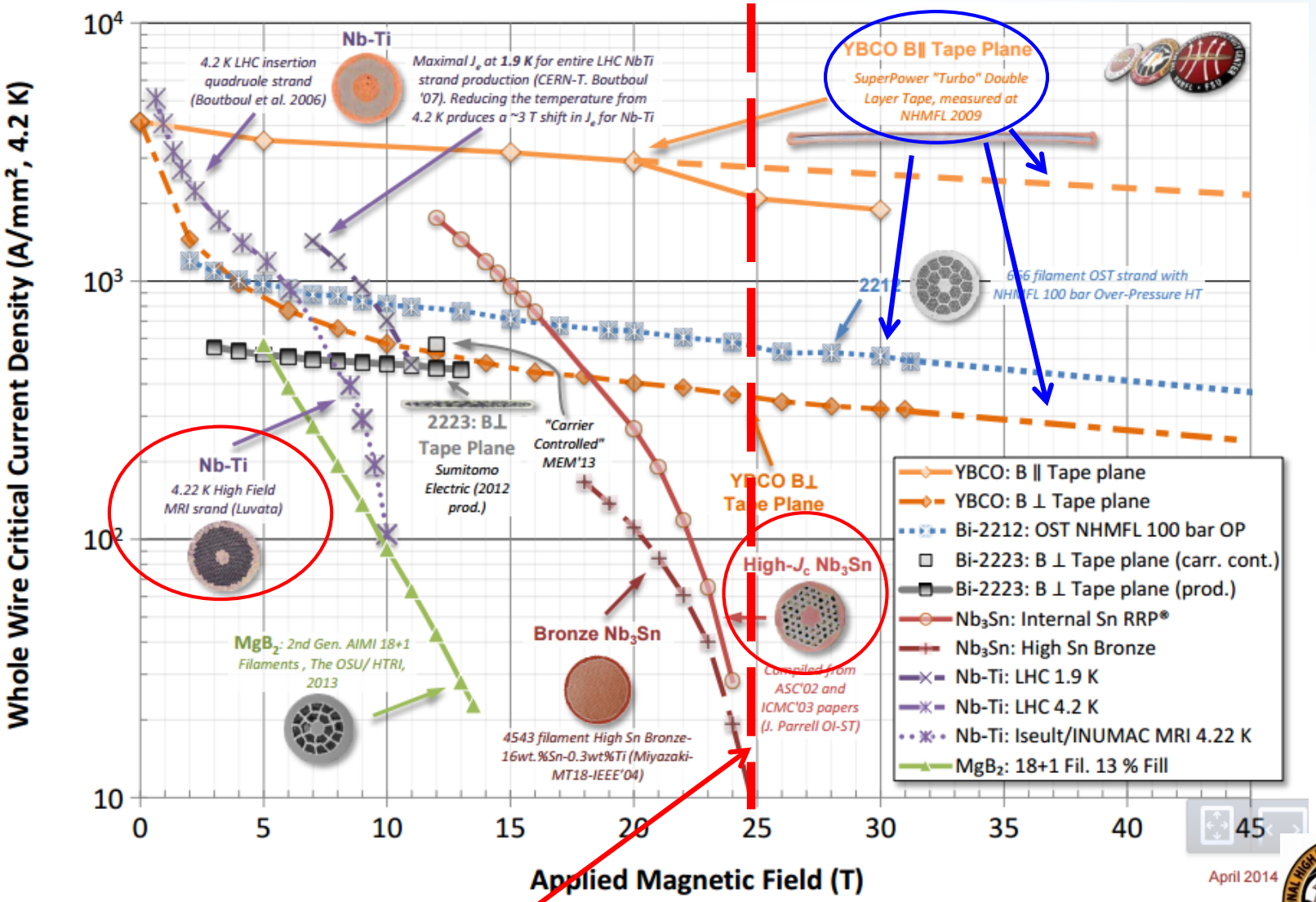

Field Limit of LTS SC Wires

Benefits with 2G-HTS REBCO Magnet

- **Huge space occupation of high-field LTS NMR magnet**
  - **Existing NMR magnet of 900 MHz or higher requiring dedicated building**
  - **2G HTS magnet enabling dramatically reduced occupation thanks to far higher Jc**

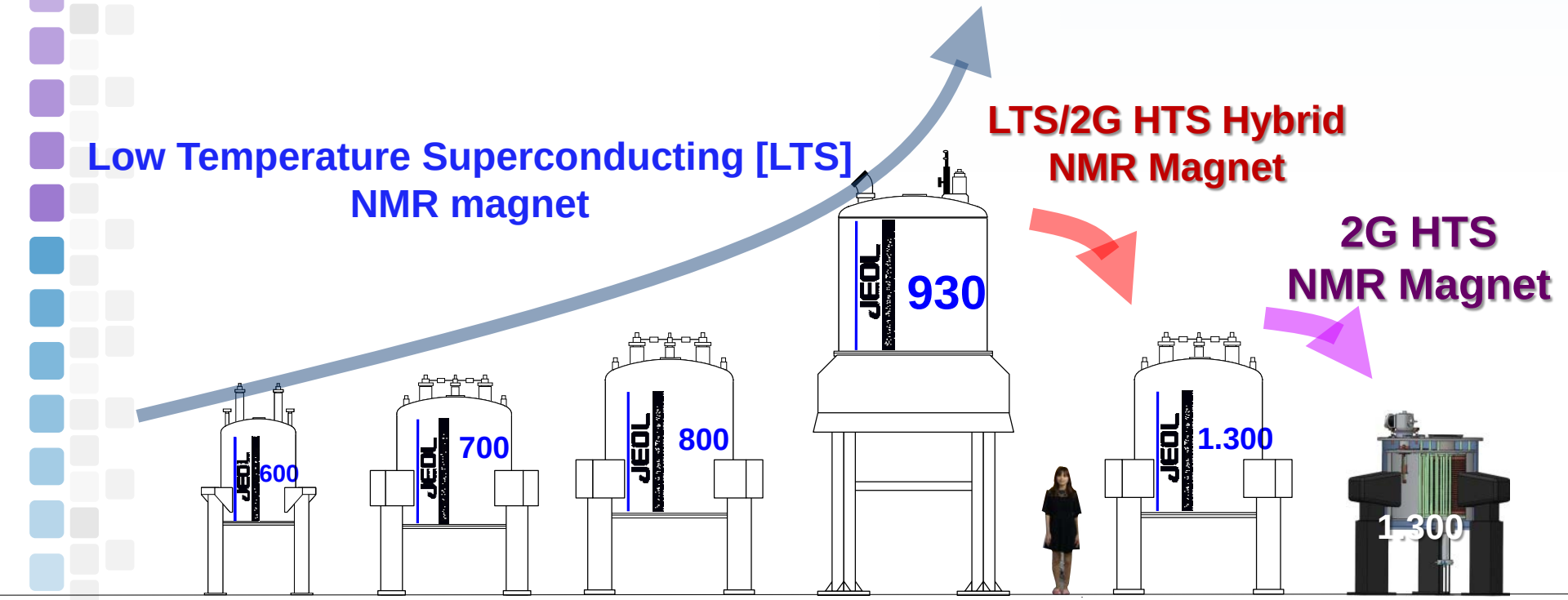

Figure in courtesy of Dr. Hideaki Maeda @ RIKEN

Development of 9.4 T 100 mm Metal-Clad NI All-REBCO NMR Magnet Embarked

- **International Collaboration**

Conduction-cooled Reduced-Vibration Cryostat

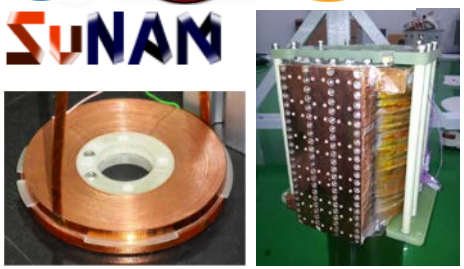

2G HTS Magnet Design, Fabrication, Evaluation & Shim

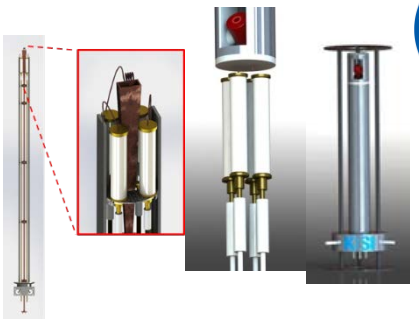

NMR Probe & Console

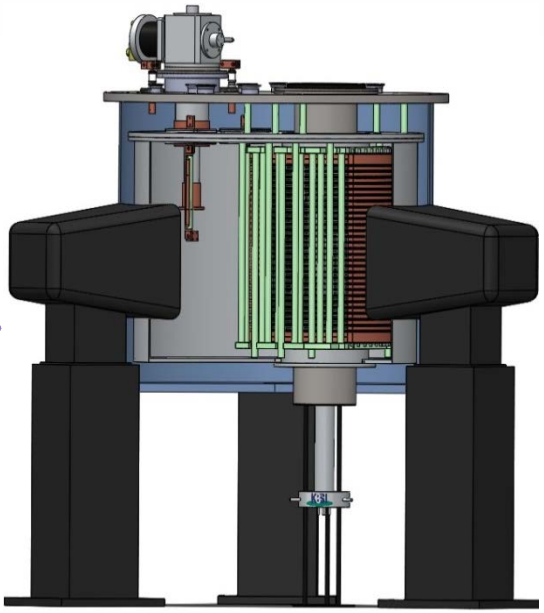

NMR System Integration & Evaluation

Benefit with No-Insulation (NI) Wiring

- When a quench occurs, the current in an NI magnet bypass the quench spot through turn-to-turn contacts from its spiral path.
- The magnet can remain safe. ➔ "self-protecting characteristic"

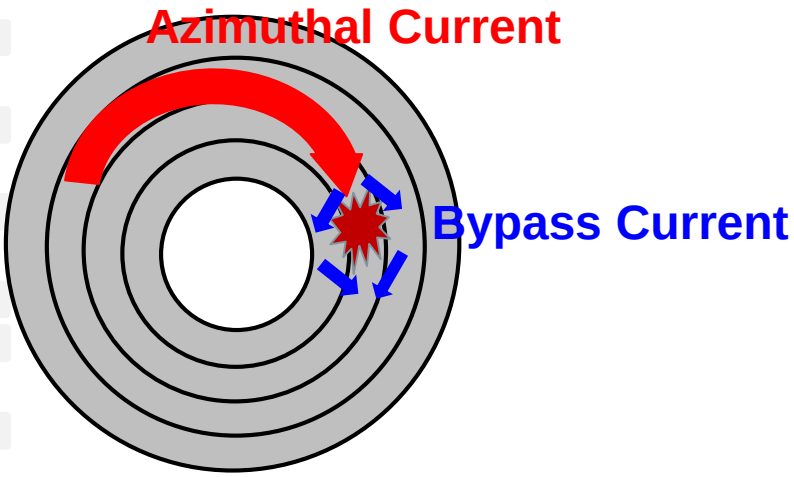

<Quench behavior in a NI coil>

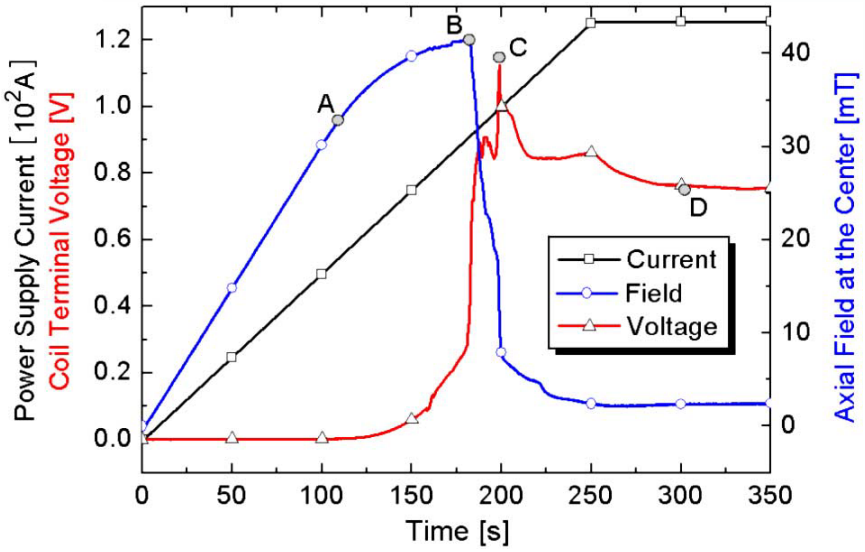

< Over current test results of a REBCO single-pancake coil up to 125 A >

REF : Seungyonh Hahn, Dong Keun Park, Juan Bascunan and Yukikazu Iwasa, "HTS Pancake Coils Without Turn-to-Turn Insulation", IEEE Trans. Appl. Supercond., vol. 21, no. 3, 1592-1595, June 2011

Benefit with Metal-Clad NI Wires

- Although the NI winding technique makes REBCO coils more robust and effective, the charging delay of the magnetic field remains a major issue.
- To tackle this charging delay issue, a 1-um thin stainless steel layers is clad on to SuNAM's REBCO tapes. stainless steel layer increase the contact resistance of the NI coil and reduce the charging delay.

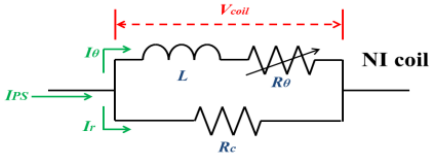

< stainless-steel-clad GdBCO tape >

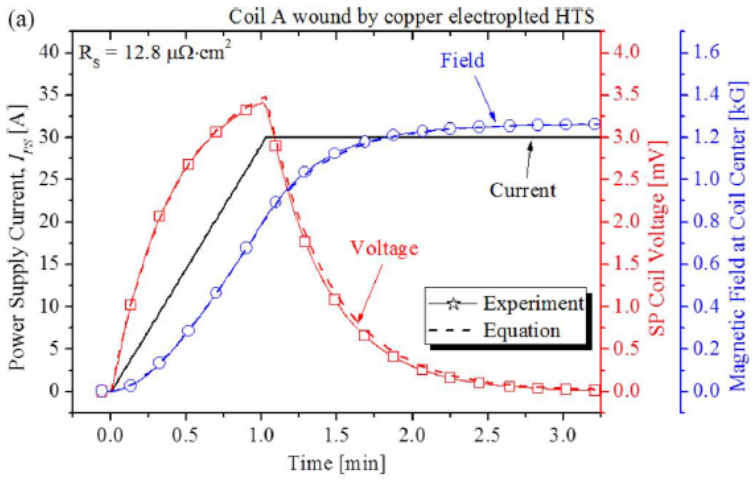

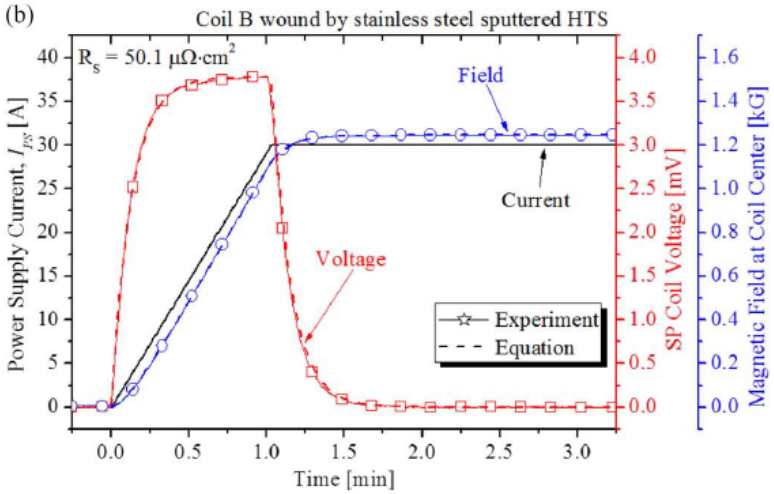

- Charging characteristics (a) without metal cladding (b) with metal cladding

REF : Jaemin Kim, Sangwon Yoon, Kyekun Cheon, Kang Hwan Shin, Seungyong Hahn, Dong Lak Kim, SangGap Lee, Hunju Lee, Seung-Hyun Moon, "Effect of Resistive Metal Cladding of HTS Tape on the Characteristic of No-Insulation Coil", IEEE Trans. Appl. Supercond., vol. 26, no. 4, 4601906, June 2016

Challenge with 2G HTS Tapes

- Screening-current induced field (SCF) generated during charging
  - SCF hurts HTS magnets' performance in temporal stability and spatial uniformity severely.
  - Mitigation of SCF is critically important for successful development of 2G HTS NMR magnet.

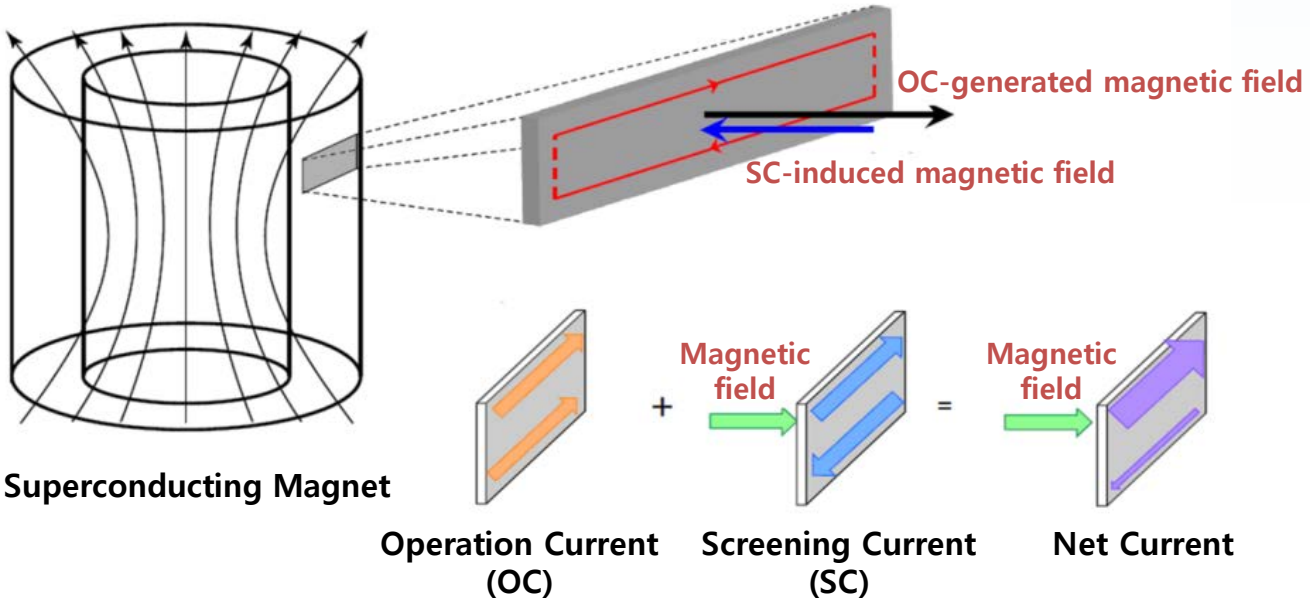

SCF degrades magnetic field's stability and uniformity of 2G HTS magnet.

REF : E. H. Brandt, et al., "Shaking of the critical state by a small transverse ac field can cause rapid relaxation in superconductors," Supercond. Sci. Technol., 2004

Progress of 9.4 T Metal-Clad NI NMR Magnet

- "NI and MW conduction-cooled metal-clad all-REBCO magnet" for 400 MHz (9.4 T) NMR (KBSI-SuNAM-NHMFL-KIMM-KNU-SNU)
  - The magnet was designed by NHMFL (May, 2016) and is under construction by the SuNAM. The magnet is about to be installed and tested at KBSI.
  - High homogeneous NMR magnet: field homogeneity is targeted lower than 1 ppm (10mm DSV) with ferro-shims and an active RT shim.
  - Metal-clad NI and MW technique ensuring self-protecting and enhanced field performance

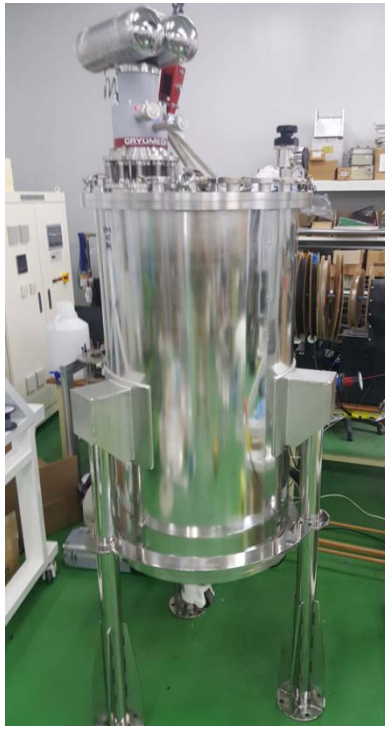

Design Parameters	
HTS conductor	SuNAM ReBCO
Magnetic field	> 9.4 [T]
Operating temperature	< 20 [K]
Operating current	187.36 [A]
Inductance	8.5 [H]
Magnet inner diameter	100 [mm]

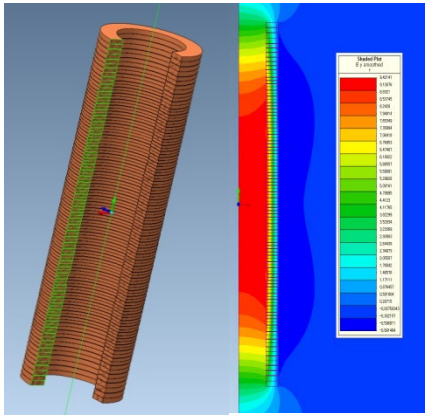

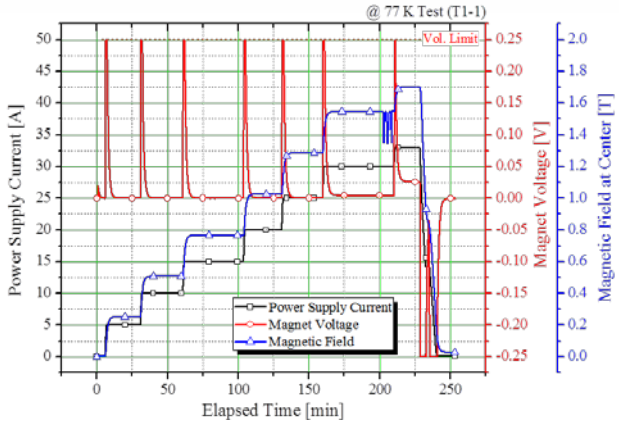

1.7T @77K

[자석 충

⇒ 현재 **1.7T** 달성(액체질
결과 비정상 **DPC** 일부

REF 1: K. L. Kim, S. Yoon, K. Cheon, J. Kim, H. Lee, S. Lee, D. L. Kim and S. Hahn, "400-MHz/60-mm All-REBCO Nuclear Magnetic Resonance Magnet : Magnet Design," IEEE Trans. Appl. Supercond., vol. 26, no. 4, 4302604, June 2016

DEMO : 3 T 100 mm MC-NI All-REBCO Magnet

- Delivered a 3 T 100 mm MC-NI All-REBCO Magnet, as a proto-type , called DEMO (Feb. 2016).
- Designed by NHMFL (May, 2015), constructed by SuNAM & KIMM, and tested by KBSI
- Under field-mapping and ferro-shimming by KBSI and Kunsan Nat'l Univ. : field homogeneity was ~500 ppm (10mm DSV) as fabricated and currently much lower than 100 ppm (10mm DSV).
- Resistive metallic-cladding NI technique applied because we expected radial resistance to shorten the charging delay while NI maintaining the self-protecting characteristic of the magnet
- Multi-width (MW) technique applied to significantly enhance the overall current density of a magnet
- First-ever attempt to verify the feasibility of metal-clad NI all-REBCO magnet as a large-scale high-field DC user magnet
- Composed of 32 double-pancake coils conduction-cooled by a two-stage pulse tube cryo-cooler

< stainless-steel-clad GdBCO tape >

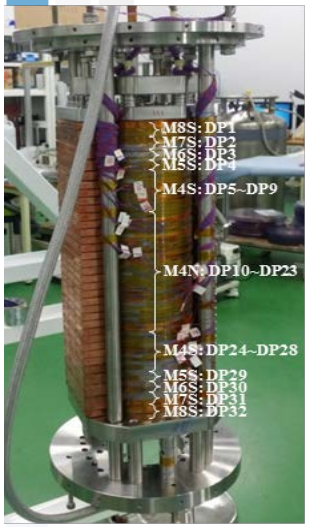

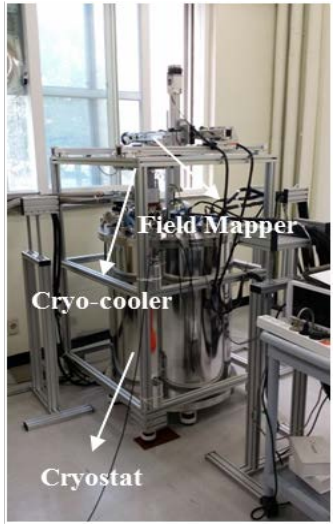

Parameters	
HTS conductor	SuNAM GdBCO
Magnetic field	> 3.0 [T]
Operating temperature	< 20 [K]
Operating current	201 [A]
Inductance	0.465 [H]
Warm bore diameter	64 [mm]

< Spec of DEMO >

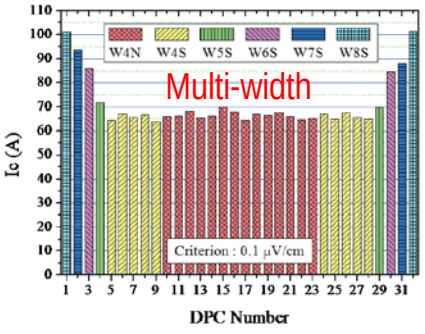

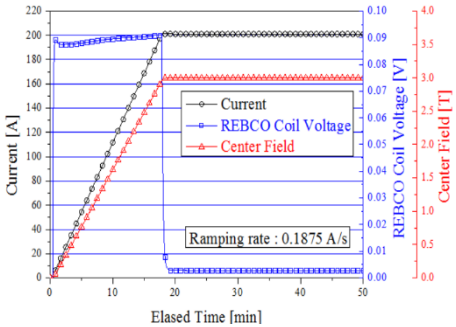

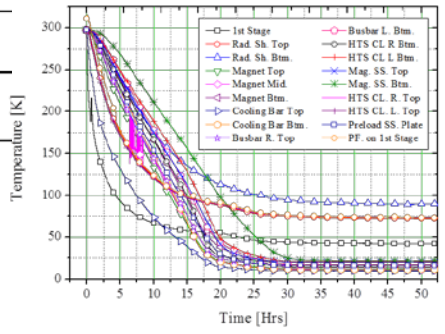

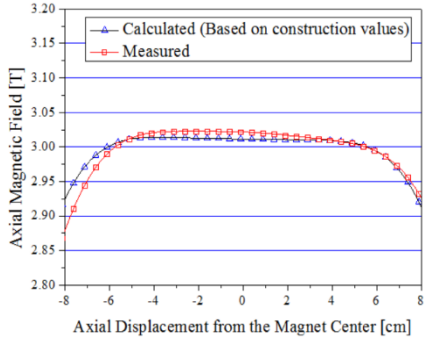

REF 1: Y. J. Hwang et al., "A Study on Mitigation of Screening Current Induced Field with a 3-T 100-mm Conduction-Cooled Metallic Cladding REBCO Magnet," IEEE Trans. Appl. Supercond., vol. 27, no. 4, 4701605, June 2017

Charging Delay Suppression during Field Ramping

- Charging delay reduction in 3 T MC magnet
  - Charging delay during field ramping is an intrinsic drawback of the NI magnet. MC technique substantially reduces the charging delay.
  - Charging time constant (L/R) of the MC magnet is 13 times smaller than that of its NI counterpart.

➔ Calculated R_{ct} of MC magnet : about 130 [μΩ·m^2]

➔ Calculated R_{ct} of NI counterpart magnet : about 10 [μΩ·m^2].

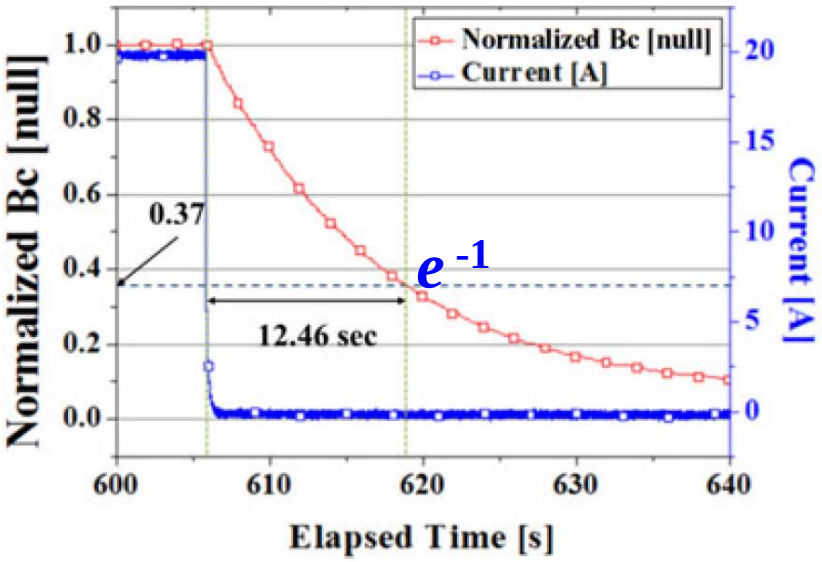

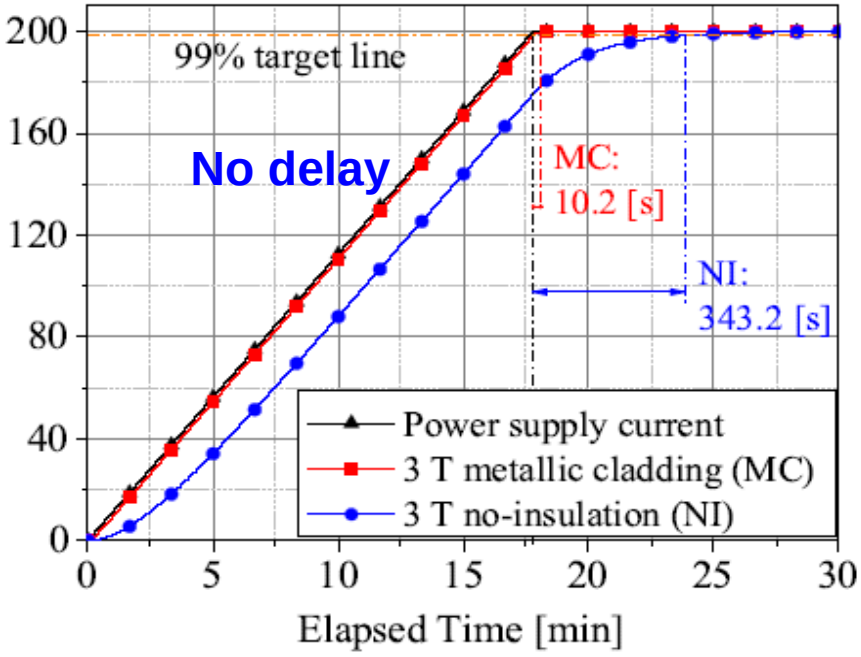

[Comparison of charging delay between the 3 T MC magnet and its NI counterpart]

Precision Field Mapping by NMR

- Mapping the magnetic field in 3-D space using an NMR spectrometer and a 3-D linear positioner.
- Using a small volume of NMR-active sample to increase a field resolution, a high-Q tank circuit, and a high-power RF amplifier for high precision measurement.

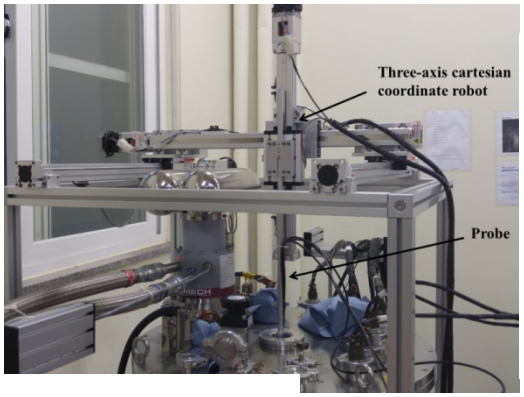

ed linear positioner >

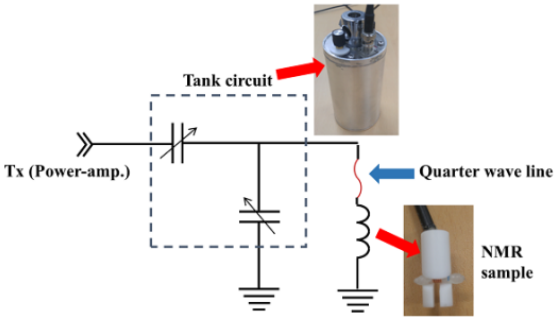

< high-Q tank circuit >

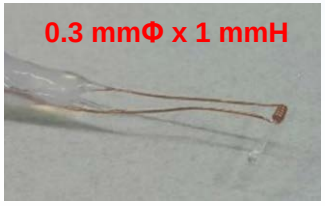

< NMR sensor >

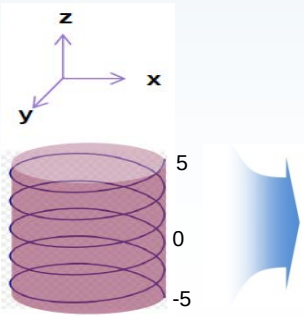

Dia. 15mm
Height 30mm
6 revolutions

< mapping pathway >

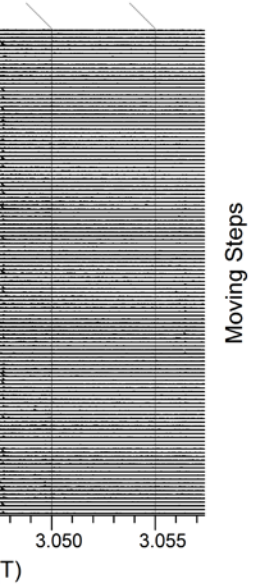

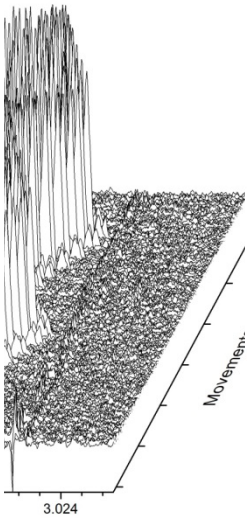

< NMR data >

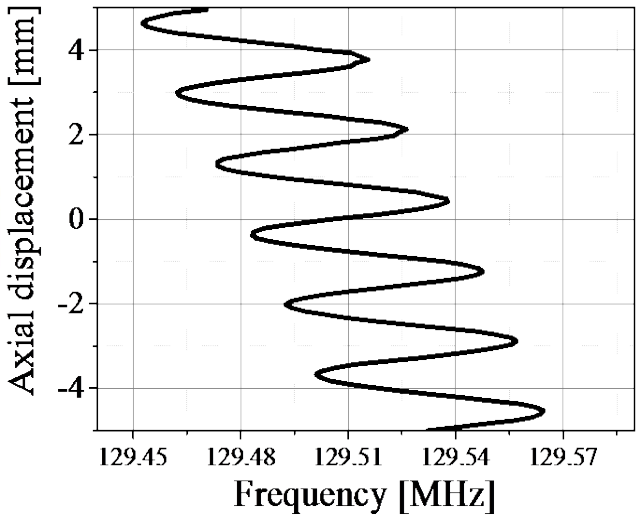

< magnetic fields along the pathway >

Z0	128.67987	MHz
Z1	-64864	Hz/cm
X	-25126	Hz/cm
Y	-54772	Hz/cm
Z2	-23017	Hz/cm^2
ZX	-5730	Hz/cm^2
ZY	2856.5	Hz/cm^2
C2	217.98	Hz/cm^2
S2	5704.2	Hz/cm^2
Z3	-1274.7	Hz/cm^3
Z2X	7493.2	Hz/cm^3
Z2Y	432.1	Hz/cm^3
ZC2	2504.5	Hz/cm^3
ZS2	-2659.3	Hz/cm^3
C3	-407.26	Hz/cm^3
S3	1553.5	Hz/cm^3

< calculated field gradients >

Evaluation of Ferro-shim for DEMO

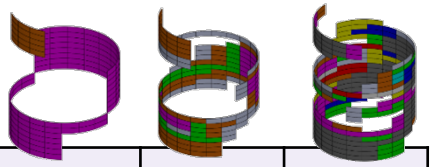

	Before Shim	1st shim	2nd shim	3rd shim
Z0 (MHz)	129.74	129.52	129.63	129.54
Z1 (Hz/cm)	**-53071.1**	-17959.7	-12847.8	**-6404.1**
X (Hz/cm)	**27148.4**	-23298	-1578.1	**3969**
Y (Hz/cm)	**-72899.9**	-2638.5	-4483.8	**-968.4**
Z2 (Hz/cm^2)	**-5580.4**	15329.9	15410.2	**-1599.2**
ZX (Hz/cm^2)	-7861.6	-16928.6	-15283.5	-12021.7
ZY (Hz/cm^2)	-1776.1	14596.8	18864	18719.2
C2 (Hz/cm^2)	-4948.9	-397.4	11407.8	-1585.2
S2 (Hz/cm^2)	2491.8	-752.9	-4594.6	7601.9
Z3 (Hz/cm^3)	-2787.2	-1358.4	-7905.4	2414.4
Z2X (Hz/cm^3)	3619.1	32133.6	23403.9	13775
Z2Y (Hz/cm^3)	2718.2	-32006.1	-27592.6	-14525.3
ZC2 (Hz/cm^3)	2537.7	7721.9	1627.2	4030.8
ZS2 (Hz/cm^3)	1864.7	3661.8	-299.3	-2392.1
C3 (Hz/cm^3)	-2214.6	4041.1	-2758.5	-2067.6
S3 (Hz/cm^3)	971.4	753	1625	3293.5
Uniformity (ppm)	**634**	262	195	**113**

<Field gradients before & after ferro-shimming>

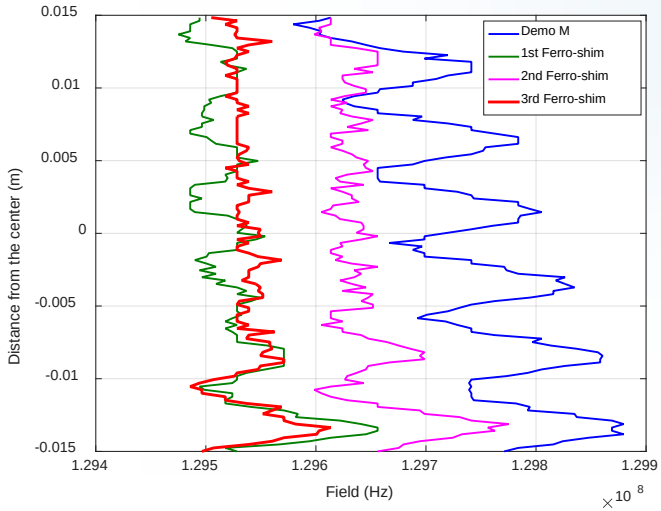

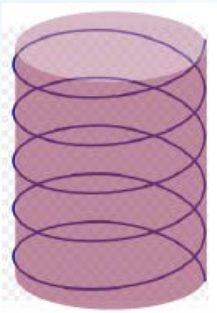

<Field map on a cylindrical helix (Φ17mm/30mm(height))>

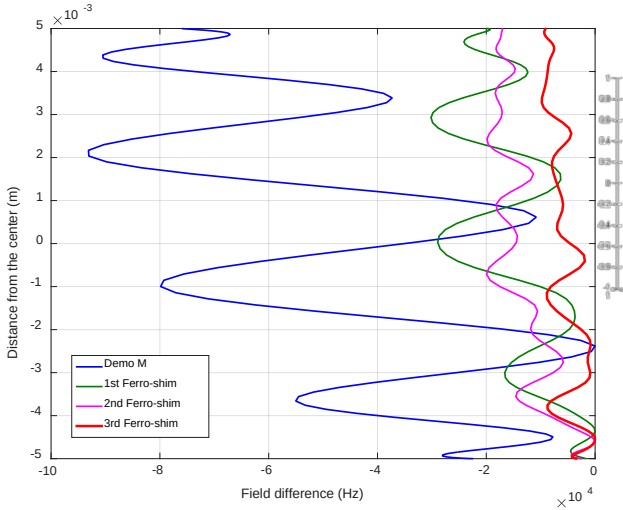

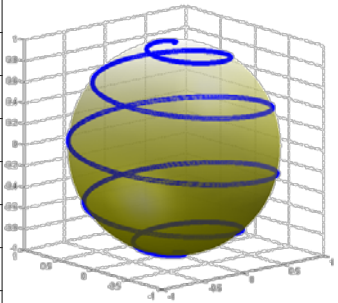

Blue: 634 ppm
Red: 113 ppm

<Field map on a spherical helix (Φ10mm DSV)>

10mmDSV inhomogeneity
634 ppm → 113 ppm (implemented as of Dec. 2017)
→ lower than 50 ppm (currently)

Need for NMR Magnetometer

- Need for a highly accurate magnetic field measurement system
  - To evaluate improvement of the magnet's field homogeneity resulting from shimming
  - To measure drift behavior of the magnetic field by long-term relaxation of screening currents induced during charging which is one of the big issues to tackle in the NMR application of REBCO wires
- Use and evaluation of the developed NMR spectrometer as a magnetometer

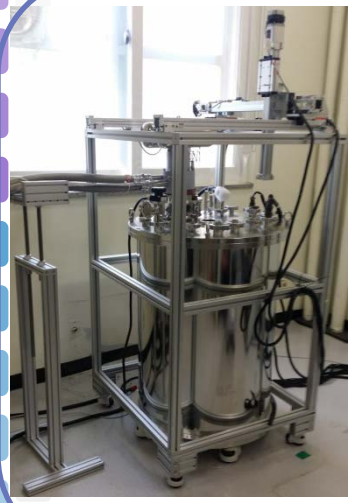

[3T DEMO]

[NMR spectrometer]

NMR detect

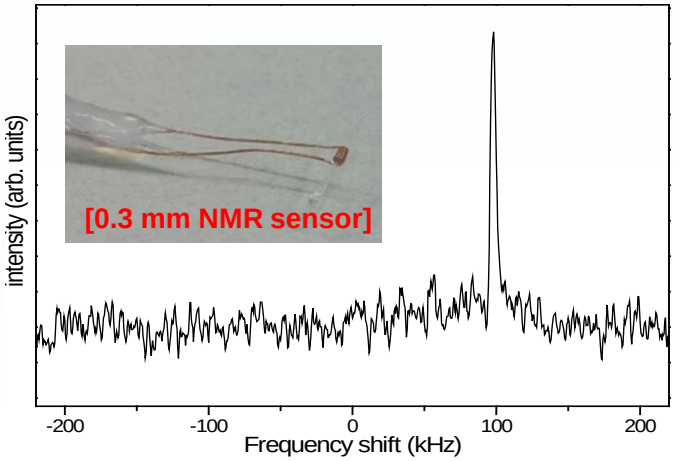

[128MHz (3T) 1H NMR spectrum of water]

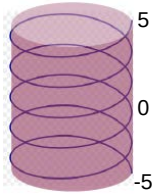

Dia. 10mm
Height 10mm
6 revolutions
<Mapping path>

NMR magnetometer_helical.avi

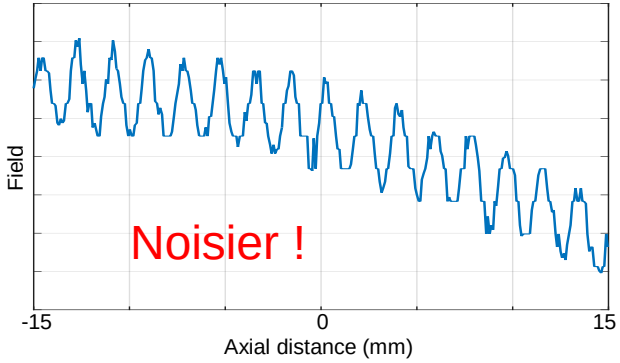

< Hall magnetomter measured >

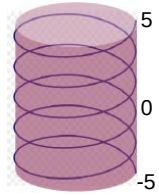

Dia. 15mm
Height 30mm
16 revolutions
<Mapping path>

Reproducible Field Gradient during Ferroshimming

- After installation of ferro-shims, CSC technique was applied to reduce the SCF.
- Field mapping was repeatedly carried out to obtain a temporal dependence of field gradients with a stack of ferro-shims. Due to the efficient reduction of SCF due to metallic cladding, calculated field gradients and homogeneity are almost the same with respect to trials.

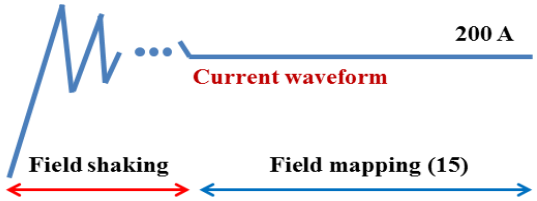

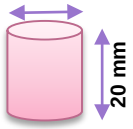

✓ **Magnetic field mapped along a helical path**

	1	3	5	7	9	11	13	15	AVG(15)	STDEV(15)
Z0	128744467.8	128744142.1	128743820.5	128744494.2	128744159.7	128743592.1	128744391.3	128744287.7	**128744177**	**502.85**
Z1	-4618.034138	-4083.231239	-3535.069854	-3768.241999	-3936.264958	-4195.9413	-3586.994288	-4182.42844	**-3942.45**	**479.02**
X	-2487.071247	-2151.704997	-2583.002607	-2571.300943	-2576.956967	-2525.949353	-2662.33075	-2734.488761	**-2530.21**	**140.81**
Y	-2672.842903	-2823.641415	-2062.980745	-2285.573645	-2621.800293	-2555.256442	-2685.54293	-2588.247302	**-2573.06**	**192.76**
Z2	2306.850233	2115.364544	1548.363098	2303.890235	2102.948028	2573.789657	2716.740427	2330.454221	**2128.6**	**464.29**
ZX	2429.750461	2216.615921	2425.374885	2610.581484	2696.021375	2710.077602	3232.731347	2868.288913	**2596.91**	**243.91**
ZY	-4303.722974	-4224.278353	-4796.958478	-4672.536315	-4566.379438	-4566.288191	-4630.937042	-4761.185653	**-4407.95**	**351**
C2	-2249.980085	-2156.014527	-2687.643976	-2460.838752	-2306.19723	-2360.100535	-2211.42948	-2382.889955	**-2305.78**	**150.88**
S2	-1464.120664	-994.2018592	-1579.872276	-1803.853536	-1583.806529	-1573.428377	-1548.659164	-1633.676705	**-1484.63**	**200.5**
Z3	-2088.23214	-1645.574903	-102.7588523	-686.2650618	-1146.329121	-1159.92464	-618.5493891	-999.7419192	**-898.57**	**842.83**
Z2X	4963.403984	4749.590825	5088.412237	4910.282462	4534.289252	4540.867433	5461.40804	4236.778007	**4713.18**	**411.46**
Z2Y	8297.882114	7945.928861	6793.303461	7433.8796	8255.146906	8057.418961	9159.555309	8267.92822	**7923.29**	**718.54**
ZC2	2418.740185	2513.968455	2666.874437	2434.674363	2454.150881	2390.343367	2689.073438	2378.408774	**2437.58**	**277.78**
ZS2	-2035.695961	-2484.177664	-1880.868339	-1869.089584	-1872.948459	-1882.236989	-1364.171753	-1809.538526	**-1939.39**	**262.23**
C3	490.2646854	65.77908892	667.2197366	810.0150056	610.0205076	577.591893	631.9026994	506.9709147	**526.9**	**193.11**
S3	-1086.868949	-1232.735984	-1445.080631	-926.8676727	-1133.701609	-1074.717024	-967.5779229	-1048.410623	**-1106.17**	**165.59**

ppm@1cm	65	60	57	61	63	64	63	64	61.9	3.1